

DOI:10.1002/ejic.201500225

Reactivity Diversification – Synthesis and Exchange Reactions of Cobalt and Iron 2-Alkenylpyridine/-pyrazine Complexes Obtained by Vinylic C(sp²)-H Activation

Robert Beck,^{*[a]} Sebnem Camadanli,^[a] Ulrich Flörke,^[b] and Hans-Friedrich Klein^[a]

Keywords: C–H activation / Cyclometalation / Cobalt / Iron / Nitrogen heterocycles

The reactivity of 2-alkenylpyridine derivatives with trimethylphosphane-supported iron- and cobalt-methyl adducts were investigated and provided a series of C,N-cyclometalated complexes through smooth vinyl C(sp²)-H activation. The reactions of Co(CH₃)(PMe₃)₄ with 2-vinylpyridine, 2-(1-phenylvinyl)pyridine, and 2-vinylpyrazine provided dark green crystals of the five-membered metallacycles (κ²-C,N-R₁R₂C=CH)Co(PMe₃)₃ (**1**: R₁ = C₅H₄N, R₂ = H; **2**: R₁ = C₅H₄N, R₂ = Ph; **3**: R₁ = C₄H₃N₂, R₂ = H). The oxidative addition of **1–3** with iodomethane afforded the *mer-trans* trivalent cobalt complexes (κ²-C,N-R₁R₂C=CH)Co(CH₃)I(PMe₃)₂ (**4**: R₁ = C₅H₄N, R₂ = H; **5**: R₁ = C₅H₄N, R₂ = Ph; **6**: R₁ = C₄H₃N₂, R₂ = H) in modest yields. The reaction of **2** with an additional equivalent of 2-(1-phenylvinyl)pyridine incorporated a second C,N metallacycle with an η²-bonded alkenyl moiety to provide (κ²-C,N-C₅H₄N-CH=CH)(κ³,η²-C,C,N-C₅H₄N-CH=CH₂)Co(PMe₃) (**7**). No cyclometalation was observed with 8-vinylquinoline and Co(CH₃)(PMe₃)₄, which afforded (κ³,η²-C,C,N-C₉H₆N-CH=CH₂)Co(CH₃)(PMe₃)₂ (**8**) with retention of the Co-CH₃ group; therefore, a suitable bite angle is required for C–H activation. No N coordination was observed with Fe(CH₃)₂(PMe₃)₄ and 8-vin-

ylquinoline (reductive elimination of C₂H₆), which afforded a low-valent Fe(PMe₃)₃ moiety bound in an η⁴-fashion with the exocyclic vinyl group and the *ortho*-carbon atoms to give (κ⁴,η⁴-C,C,C,C-C₉H₆N-CH=CH₂)Fe(PMe₃)₃ (**9**). In polar solvents, an equilibrium of cyclometalated 7,8-benzoquinoline exists between the *mer-trans* (90%) and *mer-cis* (10%) configurations of (κ²-C,N-C₁₃H₆N)Fe(CH₃)(PMe₃)₃ (**10**). At variance with the previously reported bicyclometalation of 2-(2-naphthalene-1-ylvinyl)pyridine with iron adducts, similar reactions with methylcobalt species provided the monocyclometalated η²,σ¹-bound coordination motif (κ³,η²-C,C,N-C₅H₄N-CH=CH-C₁₀H₆)Co(PMe₃)₂ (**11**). The reaction of **11** with carbon monoxide provided the monocarbonyl complex (κ³,η²-C,C,C-C₅H₄N-CH=CH-C₁₀H₆)Co(CO)(PMe₃)₂ (**12**), accompanied by the release of the N-coordination site. The carbonylation of (κ³-C,C,N-C₅H₄N-CH=C-C₁₀H₆)Fe(PMe₃)₃ resulted in the exchange of one PMe₃ ligand with the retention of the coordination sites to generate (κ³-C,C,N-C₅H₄N-CH=C-C₁₀H₆)Fe(CO)(PMe₃)₂ (**13**). All new compounds were identified by NMR spectroscopy and structurally characterized by single-crystal X-ray crystallography (with the exception of **10** and **13**).

Introduction

Cyclometalation reactions through C–H bond activation^[1] attract a great deal of interest owing to their relevance to the selective activation and functionalization of hydrocarbons and their applications in homogeneous catalysis.^[2] In particular, remarkable progress has been shown recently for cobalt-catalyzed transformations.^[3] Cyclometalated compounds have also found numerous applications^[4] in several fields such as organometallic synthesis,^[5] biologically active compounds,^[6] and materials science.^[7] Re-

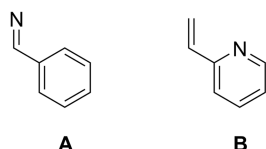
cently, cyclometalated 2-phenylpyridine derivatives of Pt and Ir showed unique features as white organic light-emitting diodes (WOLEDs) for future flat-panel display technologies.^[8] Remarkably, little information is available about the reactive intermediates that facilitate the catalytic transformations of vinylpyridine derivatives in reactions that proceed through putative metallacycles.^[9] Our main focus on cyclometalated cobalt and iron chemistry is the relatively low cost of these compounds compared with those of their heavy congeners, Ru and Rh,^[10] which provides an impetus for their utilization in catalytic or stoichiometric transformations.^[11] Therefore, we develop new syntheses and strategies involving electron-rich, trimethylphosphane-supported methylcobalt and -iron complexes, which we have recently found to be active in C–H bond activation reactions.^[12]

CoMe(PMe₃)₄ and FeMe₂(PMe₃)₄ have been cornerstones in the development of modern cobalt and iron organometallic chemistry, and an advantage of their use is

[a] Eduard-Zintl-Institut für Anorganische und Physikalische Chemie, Technische Universität Darmstadt, Alarich-Weiss-Straße 12, 64287 Darmstadt, Germany
E-mail: metallacycle@gmail.com
http://www.chemie.tu-darmstadt.de/ac/eduardzintlinstitut_1/anorganischechemie/anorganischechemie.de.jsp

[b] Anorganische und Analytische Chemie, Universität Paderborn, Warburger Straße 100, 33098 Paderborn, Germany
Supporting information for this article is available on the WWW under <http://dx.doi.org/10.1002/ejic.201500225>.

that they release chemically inert methane, which is not expected to interfere in the reaction pathway or product formation. On the basis of our previous work on imine-directed C–H bond activation,^[13] in this paper, we show that related pyridyl complexes also promote vinylic C(sp²)–H bond activation of 2-vinylpyridine derivatives, which are related to the isoelectronic imine derivatives through their interchanged 1,4-azadiene topology (Scheme 1), and extend our investigation towards π -acceptor ligand substitution (carbon monoxide) and oxidative addition (iodomethane); we also explore the limitations of their structure and reactivity relationship (bite angle) when compared with the reactivity of the isostructural imine complexes.^[14]



Scheme 1. Interchanged 1,4-azadiene topology of structural isomers with N exchanged for CH.

The cyclometalation reactions of isoelectronic 2-phenylimine (**A**; Scheme 1) derivatives have been extensively studied with Ru,^[15] Pt,^[16] and Ir.^[17] Notably, only a few examples of cyclometalated 2-vinylpyridine derivatives (**B**) have been reported, and there are selected examples of 4d and 5d transition metals with M = Pd,^[18] Pt,^[19] Os,^[20] Ru^[21] Ir,^[22] and Au,^[23] in most cases achieved through C(sp²)–H activation to assemble complexes of the type [M(κ^2 -C,N-CH=CH-C₅H₄N)].

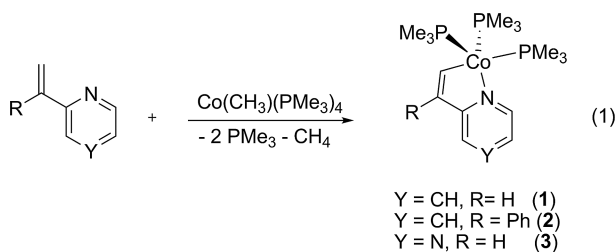
However, the reactions of first-row transition metals with 2-vinylpyridine and -pyrazine derivatives are scarce, although cobalt complexes have recently been shown to catalyze the C–C coupling reactions of 2-vinyl nitrogen-containing heteroaromatic compounds with styrylboronic acid.^[24] Mechanistically, a cyclometalated alkenylpyridine complex has been suggested as one of the key intermediates in the ruthenium-catalyzed arylation of 2-alkenylpyridines with aryl bromides.^[25]

Results and Discussion

Synthesis and Characterization of Cyclometalated 2-Vinylpyridyl Derivatives

The treatment of CoMe(PMe₃)₄ with equimolar amounts of 2-vinylpyridine,^[14] 2-(1-phenylvinyl)pyridine, or 2-vinylpyrazine at –70 °C resulted in the formation of the cyclometalated complexes (κ^2 -C,N-R₁R₂C=CH)Co(PMe₃)₃ (**1**: R₁ = C₅H₄N, R₂ = H; **2**: R₁ = C₅H₄N, R₂ = Ph; **3**: R₁ = C₄H₃N₂, R₂ = H) accompanied by the liberation of methane [Equation (1)]. Concentrated *n*-pentane solutions at –27 °C afforded almost black rhombic crystals, which dissolve in hydrocarbon solvents to produce green solutions. The ¹H NMR spectra of **1–3** in tetrahydrofuran (THF) show the absence of the cobalt–methyl protons and the appearance of a new set of signals at δ = 6.32 and 6.66 ppm

for **1**, 6.40 ppm for **2**, and 6.86 and 7.12 ppm for **3** with an upfield shift ($\Delta \approx 1.04$ ppm) compared with the signal of the free vinylic derivative.



The ¹³C{¹H} NMR spectra of **1–3** are consistent with the spectra of other transition-metal compounds containing a metalated 2-vinylpyridine ligand. In this context, it should be mentioned that the deprotonation produces an increase of electron delocalization in the five-membered ring, as demonstrated by the downfield shift of the Co–C signal ($\delta \approx 189.5$ – 192.1 ppm, for **1–3**), which provides no evidence of the carbene resonance for a significant contribution from a cobalt–alkenyl bond as found for osmium or rhenium 2-vinylpyridine complexes.^[19,21b,26] Catalytic reactions require ligand exchange reactions before carbon–carbon bond formation.^[27] The treatment of **1–3** with carbon monoxide failed to liberate stoichiometric amounts of PMe₃; moreover, we observed complete demetalation of the pyridyl backbone and the formation of dinuclear cobalt tetracarbonyl complexes (IR) and the free pyridine derivative.^[28]

Complexes **2** and **3** were isolated as green crystals suitable for X-ray crystallographic study. ORTEP depictions of these compounds are shown in Figures 1 and 2, and selected geometric values are summarized in Table 1. For five-coordinate structures, an index τ was introduced by Addison et al.^[29] to define the extent of deviation from trigonal-bipyramidal to square-pyramidal geometry ($\tau = 1$ for perfect trigonal bipyramidal; $\tau = 0$ for perfect square-based

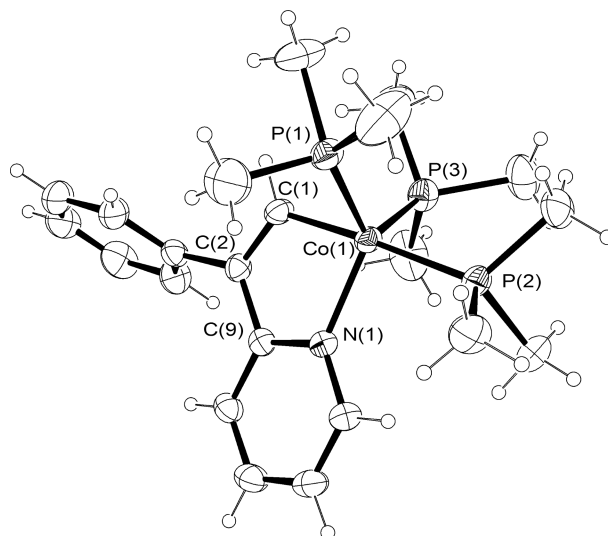


Figure 1. Depiction of the solid-state molecular structure of **2** with 50% probability ellipsoids.

pyramidal). The values for **2** ($\tau = 0.85$) and **3** ($\tau = 0.81$) indicate slight deviations from the regular trigonal-bipyramidal geometry, and the metalated carbon atom and single PMe_3 ligand occupy apical positions. The metal coordination sphere is completed by the N donor atom of the pyridyl ligand and two PMe_3 ligands in equatorial positions. The Co–P1 and Co–P2 bond lengths fall in the usual range for trimethylphosphane-stabilized cobalt(I) complexes. The molecular structures of **2** and **3** demonstrate geometric values similar to those of a manganese complex with a 2-benzocymantrenylpyridine ligand,^[30] and these complexes are the first structurally characterized cyclometalated 2-vinylpyrazine cobalt complexes.^[31]

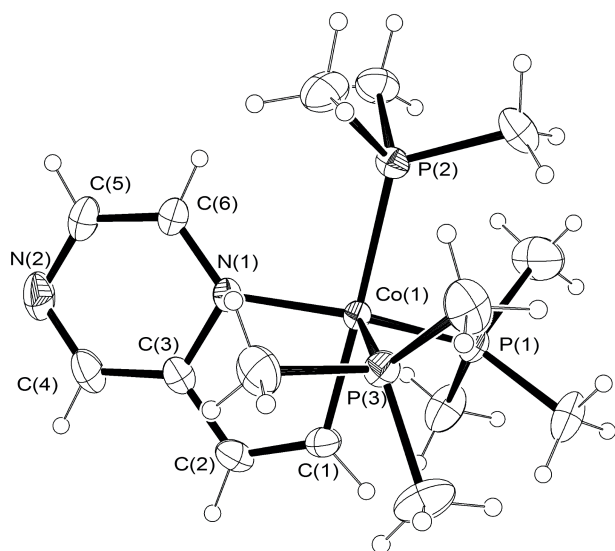


Figure 2. Depiction of the solid-state molecular structure of **3** with 50% probability ellipsoids.

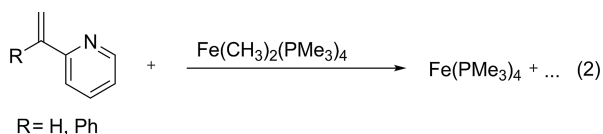
Table 1. Selected bond lengths [Å] and angles [°] of the cyclometalated Co^I complexes **2** and **3**.

	2	3
Co–C(sp ²)	1.8995(4)	1.9058(19)
Co–N	1.9919(12)	1.9428(14)
$\sigma\text{C}(\text{sp}^2)\text{--C}(\text{sp}^2)$	1.352(2)	1.348(3)
Co–P _{eq}	2.1502(5)	2.1869(5)
Co–P _{eq}	2.1708(5)	2.1761(6)
Co–P _{ax}	2.2010(4)	2.2159(5)
C(sp ²)–Co–N	80.46(6)	81.55(8)
C(sp ²)–Co–P _{ax}	176.50(5)	178.00(6)
N–Co–P _{ax}	96.24(4)	96.46(5)
P _{ax} –Co–P _{eq}	97.01(2)	96.38(2)
P _{eq} –Co–P _{eq}	112.04(2)	112.04(2)

Attempted Cyclometalation of 2-Alkenylpyridines with $\text{Fe}(\text{CH}_3)_2(\text{PMe}_3)_4$

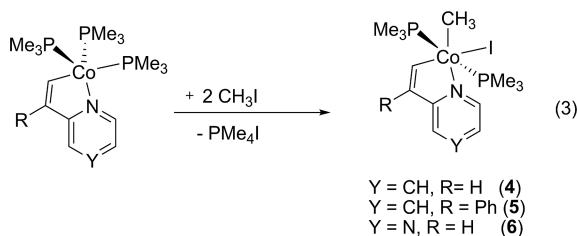
The treatment of stoichiometric amounts of 2-vinylpyridine or 2-(1-phenylvinyl)pyridine with $\text{Fe}(\text{CH}_3)_2(\text{PMe}_3)_4$ [Equation (2)] under analogous conditions as those described for $\text{CoCH}_3(\text{PMe}_3)_4$ [Equation (1)] provided low-valent $\text{Fe}(\text{PMe}_3)_4$ and ethane (C_2H_6) by reductive elimi-

nation. Additionally, ³¹P NMR spectroscopy showed the presence of a plethora of unidentified byproducts and the absence of the typical triplet/doublet spin-pattern expected for a cyclometalated iron metallacycle in an octahedral coordination sphere.^[13]



Reactions with Iodomethane

With iodomethane, the interesting question is whether the attack by the cobalt species would proceed as a regioselective addition or promote ring opening through a subsequent reductive C–C coupling reaction,^[32] as observed for related iron–imine complexes.^[13] Within 2 h, the reaction mixture turned orange-brown, and a white precipitate of tetramethylphosphonium iodide indicated that the reaction proceeded according to Equation (3).



When excess iodomethane was used (Co/MeI ca. 1:5), large amounts of decomposition products were isolated such as $\text{CoI}(\text{CH}_3)_2(\text{PMe}_3)_3$ ^[33] and $\text{CoI}(\text{PMe}_3)_3$.^[34] Additionally, a small amount of a third byproduct demonstrated by a singlet ¹H NMR resonance at $\delta = 2.35$ ppm, typical for an Ar–CH₃ derivative, suggests that intramolecular reductive C–C coupling of the Co–CH₃ moiety and the pyrazyl backbone of **6** occurs to form a methylated pyrazine derivative. Unfortunately, crystals suitable for X-ray diffraction could not be obtained to verify this suggestion. The solution IR and NMR spectroscopic data for all new compounds [e.g., IR: $\tilde{\nu} \approx 1162\text{--}1157\text{ cm}^{-1}$ $\delta_{\text{as}}(\text{Co--CH}_3)$; ¹³C{¹H} NMR: $\delta = 184.5$ ppm (m, Co–C=C); ¹H NMR: $\delta \approx 0.30\text{--}0.45$ (t, ³J_{P,H} ≈ 10 Hz, Co–CH₃)] enabled the stereochemical assignments for **4–6**; in particular, the ³¹P{¹H} NMR spectra all manifested singlets, consistent with a *trans* disposition of the trimethylphosphane ligands and in agreement with the X-ray structural determination (Figures 3 and 4) of approximately octahedral geometries for **4–6** in the solid state. These structures are closely related to five-membered imine cobaltocycles, in which a strong *trans* influence of the methyl group is recognized. The upfield range in the ¹H NMR spectra for the Co–CH₃ resonances of **4–6** is diagnostic that the methyl group is *trans* to the nitrogen}

donor. Crystals of **5** and **6** are stable in air for more than two hours and could thus be mounted on an X-ray diffractometer without inert-gas protection. The X-ray structure determination data were obtained from low-temperature measurements under a N₂ stream to provide high-quality X-ray parameters (Table 5). The molecular structure of **5** (Figure 3) confirms the octahedral configuration derived from the spectroscopic data. The iodo and methyl ligands lie in the plane of the chelate ring, and the two Co–C bonds are mutually *cis* [C7–Co1–C8 92.20(17)°]. The trimethylphosphane ligands approximately eclipse each other, as indicated by their idealized mirror symmetry with respect to the Co–I and Co–C bonds. Both PMe₃ ligands appear slightly bent [P2–Co1–P1 171.81(5)°] towards the Co–CH₃ group. This bending and the bite angle of the

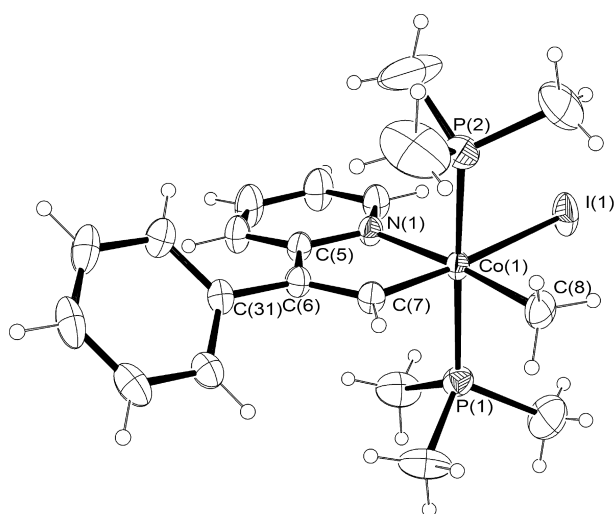


Figure 3. Depiction of the solid-state molecular structures of **5** with 50% probability ellipsoids.

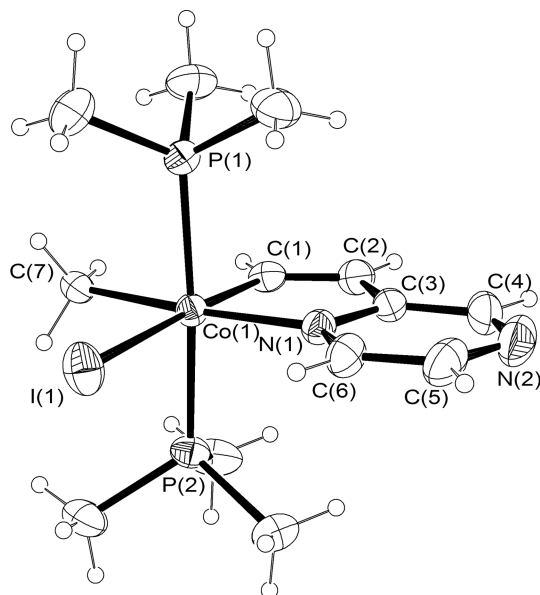


Figure 4. Depiction of the solid-state molecular structures of **6** with 50% probability ellipsoids.

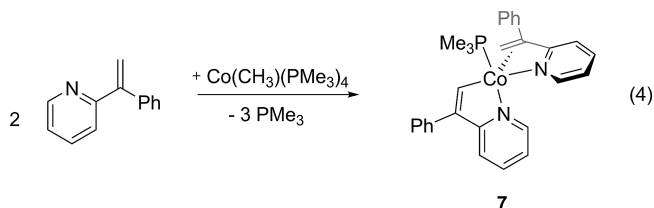
chelating ligand [C7–Co1–N1 81.02(13)°] reflect the spatial requirements of the iodo ligand. The sum of the internal angles (539.8°) indicates a slightly distorted five-membered metallacycle. The strong *trans* influence of the Co–CH₃ group in **5** causes an elongation of the Co1–N1 bond by 0.045 Å compared with that of the corresponding parental cobalt complex **2**. Remarkably, the Co–N bond lengths for **2**, **3**, **5**, and **6** are ca. 0.10–0.15 Å shorter when compared with those of a related square-based pyramid configuration, which might be attributed to the missing *trans* nitrogen donor ligand of this complex.^[35] The Co–C(sp³) bond length of **5** [2.015(4) Å] is 0.145 Å longer than the average distance between cobalt and aryl carbon atoms but still in the range of cobalt–carbon distances reported previously.^[36] The structural values determined for **5** closely resemble those of the 2-vinylpyrazyl derivative **6** (Figure 4, Table 2).

Table 2. Selected bond lengths [Å] and angles [°] of the methyl–Co^{III} complexes **5** and **6**.

	5	6
Co–C(sp ²)	1.875(3)	1.874(3)
Co–C(sp ³)	2.015(4)	2.077(3)
Co–N	2.037(3)	2.024(2)
σC(sp ²)–C(sp ²)	1.341(5)	1.332(4)
Co–I	2.6943(5)	2.7214(5)
Co–P1	2.2165(11)	2.2194(9)
Co–P2	2.2078(12)	2.2229(9)
C(sp ²)–Co–N	81.02(13)	81.42(13)
C(sp ²)–Co–C(sp ³)	92.20(17)	91.30(13)
C(sp ²)–Co–I	175.15(10)	174.98(10)
N–Co–I	94.46(8)	93.59(7)
P1–Co–P2	171.81(5)	172.04(4)

Subsequent Double Vinylic Activation of C₆H₄N(Ph)–C=CH₂

The treatment of CoMe(PMe₃)₄ with 2 equiv. of 2-(1-phenylvinyl)pyridine in *n*-pentane under ambient conditions for 2 h is accompanied by the release of methane and three trimethylphosphane ligands to afford the dark brown complex **7**, which is isolated in 83% yield [Equation (4)]. Similarly, **2** is converted to **7** with 1 equiv. 2-(1-phenylvinyl)pyridine, as monitored by NMR spectroscopy. Remarkably, the analogous reaction with 2 equiv. of 2-vinylpyridine failed to form a similar complex owing to its weaker π-backbonding ability.^[37]



We found no evidence of a second isomer containing the η²-bound vinyl substituent of the 2-(1-phenylvinyl)pyridine ligand in *anti* fashion, as previously reported for the reac-

tion of $\text{OsH}_2\text{Cl}_2(\text{P}i\text{Pr}_3)_2$ with 2-vinylpyridine.^[38] Dark brown cubic crystals of **7** were obtained by recrystallization from *n*-pentane solution at -27°C . Solid **7** can be handled at room temperature for days without significant decomposition; however, solutions decompose over weeks at room temperature, and cobalt metal is deposited. Complex **7** contains two substrate molecules. One of them is metalated, as a consequence of the $\text{C}(\text{sp}^2)\text{-H}$ bond activation of the vinylic CH_2 substituent, whereas the other one is coordinated to the cobalt atom by the nitrogen atom and the $\text{C}=\text{C}$ double bond in an η^2 fashion. In agreement with both types of coordination mode of the pyridine ligands in **7**, the $^{13}\text{C}\{^1\text{H}\}$ NMR spectrum shows two groups of vinylic resonances, those of the η^2 -coordinated substituent are typically upfield-shifted and are observed as a singlet at $\delta = 38.1$ ppm and a doublet at $\delta = 60.5$ ppm with $^2J_{\text{PC}} = 11.3$ Hz, whereas the metalated vinyl carbon atom appears as a multiplet at $\delta = 199.5$ ppm, in a similar range as that observed for the parent complex **2** ($\delta = 191.2$ ppm).

X-ray Structure Determination of **7**

Single crystals of **7** suitable for structural analysis by X-ray crystallography were directly obtained from the synthesis in *n*-pentane. An ORTEP depiction of the solid-state molecular structure is shown in Figure 5, and the X-ray crystallographic collection and refinement parameters are included in Table 5. The molecule has no symmetry; and the atoms of the σ -metalated and η^2 -bound vinyl(phenyl)pyridyl ligands lie almost in perpendicular planes, and the single PMe_3 ligand occupies an equatorial position. The bond angles around the distorted trigonal-pyramidal cobalt center ($\tau = 0.66$) are close to 90° , and the smallest one [$77.9(1)^\circ$] involves the five-membered chelate ring. The metalated vinyl carbon atom lies *trans* to the second η^2 -bound N coordination site of the vinylpyridine ligand, and the $\text{Co}(1)\text{-C}(7)$ bond length of $1.865(3)$ Å is short compared to the usual values for vinyl carbon bonds ($1.98\text{--}2.06$ Å).^[39] There is no structural hint for agostic interactions in the void opposite the $\text{Co}(1)\text{-N}(1)$ bond, the $\text{Co}\text{-P}$ distance [$2.4134(8)$ Å] is in the typical range,^[36] and the longer $\text{Co}(1)\text{-N}(2)$ bond [$2.033(2)$ Å] compared with the $\text{Co}(1)\text{-N}(1)$ bond [$1.986(2)$ Å] reflects the strong *trans* influence of the $\text{Co}\text{-C}7$ bond, which is shorter than those of related cobalt-imine complexes ($2.11\text{--}2.12$ Å). The $\text{C}(6)\text{-C}(7)$ bond length of $1.339(4)$ Å is typical for an $\text{sp}^2\text{-sp}^2$ double bond, whereas the elongated $\text{C}(19)\text{-C}(20)$ bond of $1.457(4)$ Å reflects the metal π -coordination. The double metalated adduct **7** is related to previously reported osmium complexes^[21a,38] containing both coordination modes for the cyclometalation of 2-vinylpyridine. Remarkably, mononuclear first-row late-transition-metal species with a five-membered cyclometalated 2-vinylpyridine ligand and an additionally η^2 -bound coordination motif have rarely been structurally characterized.^[21a,22,38,40]

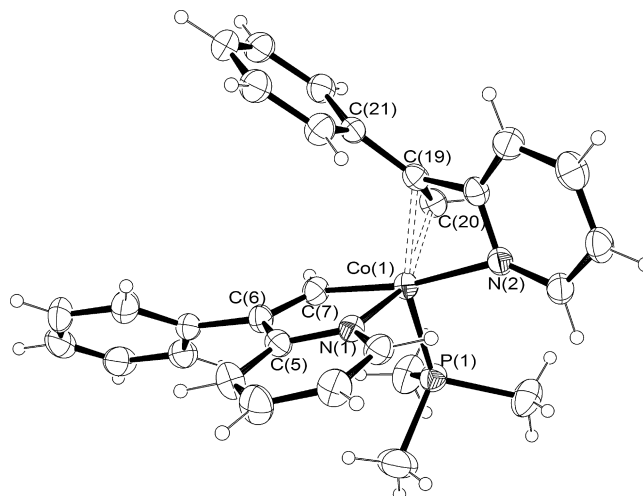


Figure 5. Depiction of the solid-state molecular structure of **7** with 50% probability ellipsoids.

To gain further insight into the electronic properties of **7**, the gas-phase structures were optimized by using three different DFT functionals, namely, PBE0, B3PW91, and M06L, in combination with the TZVP basis set. The optimized geometry and solid-state structure of **7** both possess a distorted square-planar geometry around the Co^{I} center, distinct from the more commonly observed trigonal-bipyramidal geometry found for the monocyclometalated parent complex **2**. The structural parameters of the energy-optimized structure are within 0.04 Å of those of the crystal structure, except for the carbon-hydrogen bond lengths, which as usual are systematically underestimated by ca. 0.10 Å in the X-ray diffraction results. The best results were obtained with the PBE0/TZVP level of theory (Table 3) [e.g., $\text{Co}(1)\text{-C}(7)$ in **7**: calcd. 1.86507 Å, exp. $1.865(3)$ Å]. The highest occupied molecular orbital (HOMO) of the doubly activated σ - and η^2 -vinylpyridine of **7** (Figure 6; for HOMO-1 to HOMO-4, see the Supporting Information) is mainly located at the pyridyl N-donor atom of the cyclometalated σ -vinyl substituent. The HOMO also represents

Table 3. Geometric parameters for **7** from DFT calculations [B3PW91, PBE0, M06L (TZVP)] and from the X-ray crystal structure.^[a]

Parameter ^[b]	B3PW91	PBE0	M06L	X-ray
$\text{Co}(1)\text{-C}(7)$	1.86587	1.86507	1.86523	1.865(3)
$\text{Co}(1)\text{-N}(1)$	2.01240	2.00699	2.03147	1.986(2)
$\text{Co}(1)\text{-C}(20)$	1.95834	1.94893	1.96600	1.980(3)
$\text{Co}(1)\text{-C}(19)$	2.04296	2.02746	2.03151	2.024(2)
$\text{Co}(1)\text{-N}(2)$	2.07074	2.06111	2.07676	2.033(2)
$\text{C}(6)\text{-C}(7)$	1.36088	1.35875	1.36205	1.339(4)
$\text{C}(19)\text{-C}(20)$	1.44967	1.44983	1.45003	1.457(4)
$\text{Co}(1)\text{-P}(1)$	2.19395	2.18297	2.17811	2.1648(8)
$\text{C}(7)\text{-Co}(1)\text{-N}(1)$	81.733	81.866	81.563	81.50(11)
$\text{C}(7)\text{-Co}(1)\text{-N}(2)$	164.771	164.898	164.043	167.82(11)
$\text{N}(1)\text{-Co}(1)\text{-P}(1)$	103.295	102.853	103.462	103.27(6)
$\text{N}(1)\text{-Co}(1)\text{-N}(2)$	95.961	95.929	95.204	95.17(9)
$\text{C}(20)\text{-Co}(1)\text{-P}(1)$	100.601	100.907	103.735	107.01(9)

[a] Distances in [Å] and angles in $^\circ$. [b] The atom numbering for the DFT results relate to the X-ray numbering scheme.

the main π bonding interaction between C19 and C20, which is polarized toward the Co center, whereas the LUMO is its antibonding counterpart. On the other hand, the HOMO–1 represents the remaining double bond character of the σ -coordinated 2-vinylpyridyl moiety. Overall, the electronic properties of the optimized structure of **7** obviates the incorporation of a possible Co–H species within the void opposite the N1–Co1 axis.

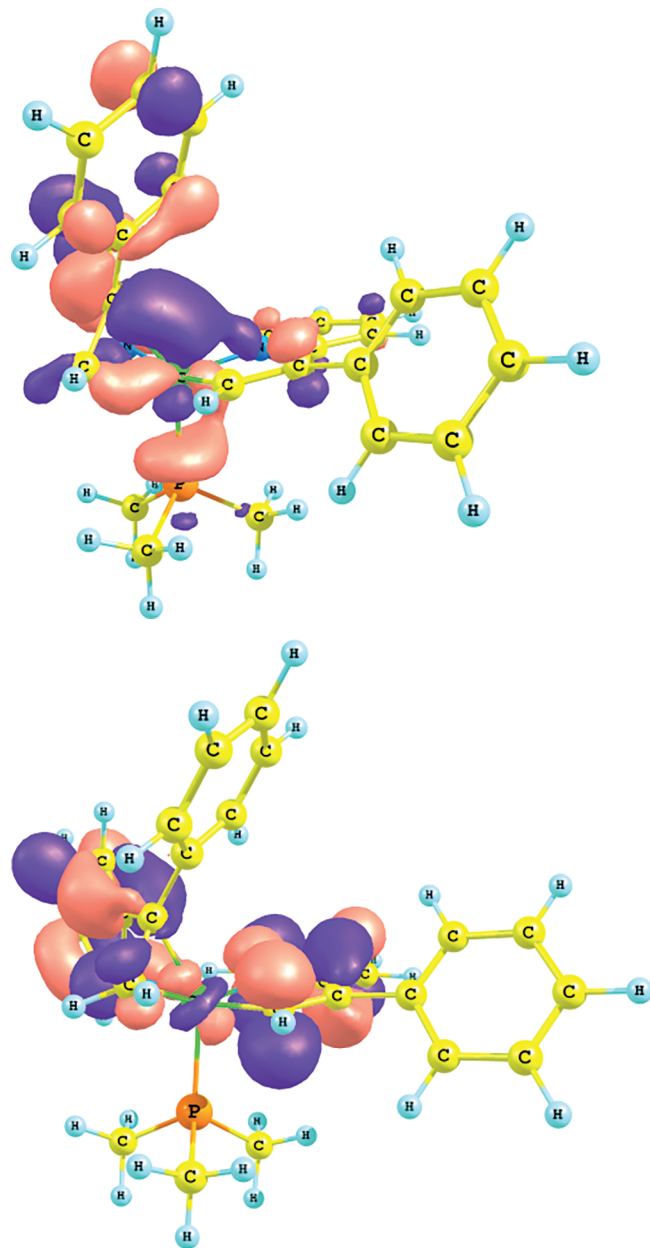
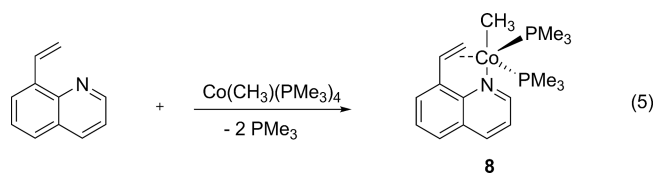


Figure 6. HOMO (top) and LUMO (bottom) of **7** as calculated by DFT (PBE0/TZVP).

Retaining a Co–CH₃ Group with 8-Vinylquinoline

We investigated further structure–reactivity relationships by using the 8-vinylquinoline ligand, which can be considered to have a flexible bite angle,^[41] in an attempt to mobi-

lize the cobalt–methyl group within cyclometalation processes for an envisaged vinylic C–H activation in a potential five- or six-membered metallacycle. The treatment of (CoMe(PMe₃)₄) in *n*-pentane at low temperature (–70 °C) with 8-vinylquinoline produced a dark violet solution and a brown precipitate, from which the η^2 -bound complex (κ^3, η^2 -C,C,N-C₉H₆N–CH=CH₂)Co(CH₃)(PMe₃)₂ (**8**) was isolated as dark violet needles in 74% yield [Equation (5)]. Complex **8** is also produced if the reaction is carried out in THF or benzene over extended reaction periods. THF solutions of CoMe(PMe₃)₄ and 8-vinylquinoline were monitored during product formation, and we found no evidence of a potential six-membered metallacycle or a possible cobalt–carbene complex,^[42] which can be conveniently obtained from the Grubbs second-generation catalyst [(H₂IMes)(PCy₃)(Cl)₂Ru=CHPh, H₂IMes = 1,3-bis-(2,4,6-trimethylphenyl)-2-imidazolidinylidene] and vinyl-substituted quinoline and quinoxaline through a ligand exchange procedure.^[43]



Additional attempts to mobilize the remaining methyl group of **8** and force cyclometalation through C–H activation failed when a benzene solution of **8** was heated to 55 °C for 4 h; therefore, the product complex is extremely stable, and only small amounts of unidentified byproducts were observed. In the IR spectrum of **8**, C=CH₂ stretching vibrations are observed at $\tilde{\nu}$ = 1568 cm^{–1}, and deformation vibrations are observed at $\tilde{\nu}$ = 1169 and 1142 cm^{–1}, as usually found for η^2 -bond alkenyl groups and cobalt-bound methyl groups, respectively. The ¹H NMR spectrum of this compound in THF at room temperature shows three characteristic upfield signals and NOE effects were observed between the η^2 -bound vinylic group and the ³¹P nuclei when this signal was irradiated. The signals of the π -coordinated Co–CH=CH₂ moiety were detected at δ = 1.93, 2.02, and 2.64 ppm, and the observation of two separated signals for the asynchronous PMe₃ ligands and the signal of the retained CoCH₃ group at δ = –1.77 as an apparent broad triplet with ³J_{P,H} = 7.2 Hz indicate high phosphane exchange mobility within the limited time scale of the spectrometer. The singlet observed in the ³¹P{¹H} NMR spectrum at δ = 15.5 ppm decoalesced below 243 K and resolved into two doublets with ²J_{P,P} = 61.3 Hz; therefore, the cobalt environment is asymmetric. The estimated free activation energy of the dynamic process is 11.4 kcal/mol.^[44] Similarly to the ¹H NMR spectrum, the ¹³C{¹H} NMR spectrum demonstrates an upfield shift of the characteristic resonance of the σ -bound Co–CH₃ group (Figure 7), which appears as a triplet at δ = –14.5 ppm with ²J_{P,C} = 12.7 Hz, whereas the resonances of the olefinic π -bound carbon atoms appear as doublets at δ = 49.7 and 53.8 ppm with ²J_{P,C} = 16.4 and 16.7 Hz, respectively, as resolved by DEPT experiments.

Remarkably, **8** is the first structurally characterized cyclo-metallated 8-vinylquinoline complex bearing an η^2 -bound vinyl group.^[31]

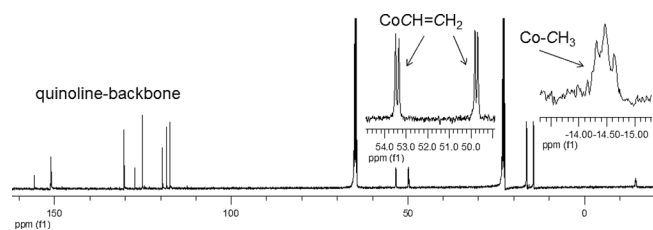


Figure 7. Experimental 125 MHz $^{13}\text{C}\{^1\text{H}\}$ NMR spectrum of **8** at 298 K in $[\text{D}_8]\text{THF}$;^[45] the expansions show the resonances of the metalated σ - and π -bound carbon atoms.

The molecular structure of **8** has been confirmed by an X-ray diffraction study. The crystallographic details as well as selected bond lengths and angles are given in Table 5. The X-ray structure shown in Figure 8 clearly reveals that the complex is a neutral, low-valent cobalt(I) molecule with two PMe_3 ligands, the remaining cobalt–methyl group, and an κ^3, η^2 -8-vinylpyridine ligand coordinated to the cobalt center through the N atom and C2 and C3 of the vinyl substituent. The complex adopts an almost perfect trigonal-bipyramidal structure ($\tau = 0.97$) with $\text{N1-Co1-C1} = 172.35(9)^\circ$ at the apical positions and with the quinolinyl backbone and the methyl group in the same plane. The $\text{CH}=\text{CH}$ vector is essentially perpendicular to the equatorial plane, that is, parallel to the Co-P bonds. The Co-C bonds [$1.982(2)$ and $1.998(2)$ Å] and the C-C bond [$1.424(4)$ Å] associated with the η^2 -bound vinyl substituent are in the typical range reported for other olefin–cobalt complexes.^[46]

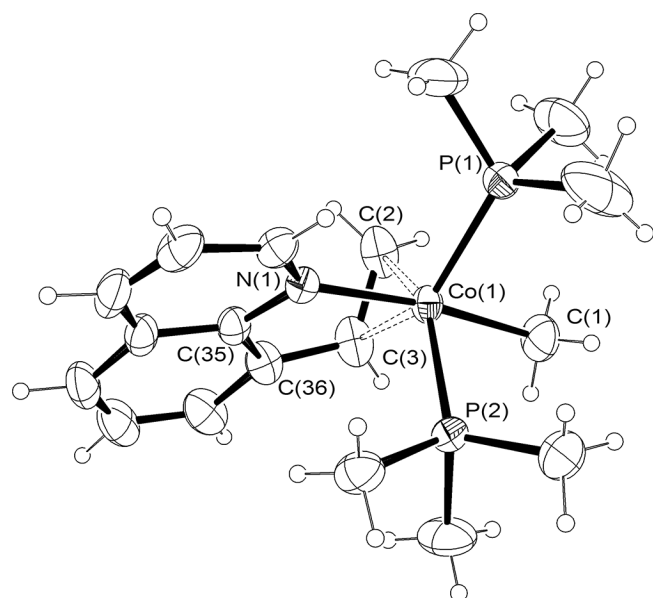
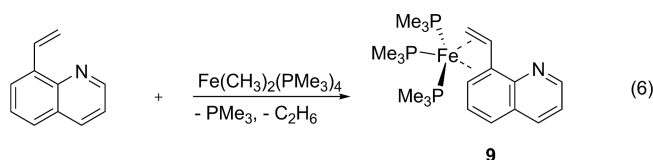


Figure 8. Depiction of the solid-state molecular structures of **8** with 50% probability ellipsoids.

Reductive Elimination through $\text{CH}_3\text{-CH}_3$ Loss from *cis*- $\text{Fe}(\text{CH}_3)_2(\text{PMe}_3)_4$

Previous reports of various aryl C–H bond activation reactions of related aryl imine^[12d,14,47] or arylaza–allylpyridine ligands^[48] with $\text{Fe}(\text{CH}_3)_2(\text{PMe}_3)_4$ prompted efforts to affect the related arylation of benzannulated pyridines, as observed with $\text{CoMe}(\text{PMe}_3)_4$ [Equation (4)]. The reaction of $\text{Fe}(\text{CH}_3)_2(\text{PMe}_3)_4$ with 8-vinylquinoline [Equation (6)] was examined even though it does not form a five-membered metallacycle through C–H activation with cobalt adducts. We were interested here in the degree to which the nitrogen donor would bind to the Fe center and whether such binding might assist the conversion of this olefin to a six-membered metallacycle or a carbene-type complex^[43,49] and give additional mechanistic insight into the previously reported conversions with closely related phenylimines.^[13] When solutions of the starting materials were combined at -70°C [Equation (6)], the reaction mixture turned dark brown within 10 min. Red-brown crystals of $(\kappa^4, \eta^4\text{-C,C,C,C-C}_9\text{H}_6\text{N-CH=CH}_2)\text{Fe}(\text{PMe}_3)_3$ (**9**) were isolated; **9** is extremely air-sensitive in solution, and crystals ignite within seconds in contact with air.



In situ ^1H NMR spectroscopy with a cold sample (-50°C) of stoichiometric amounts of *cis*- $\text{Fe}(\text{CH}_3)_2(\text{PMe}_3)_4$ and 8-vinylquinoline in $[\text{D}_8]\text{THF}$ showed first the exchange of one PMe_3 ligand, and the pyridyl N donor ligand was preferred over the vinylic group. A stable iron dimethyl complex through *N*-pyridyl coordination was recently established in our work with 2-benzoylpyridine.^[50] In the NMR spectra, increased line broadening is observed. The resonances of both separated methyl groups arise as broad singlets in the ^1H NMR spectrum ($\delta = -1.11$ and 0.59 ppm). Afterwards, the intact dimethyl moiety converts within minutes through the reductive elimination of ethane instead of Ar-CH_3 elimination, and the released trimethylphosphane-supported Fe^0 source prefers exocyclic η^4 -bound aryl/vinyl coordination rather than the coordination of the pyridyl donor linkage. By contrast, we previously observed a regioselective C–H activation preceded by a $\text{Csp}^2\text{-Csp}^3$ elimination product (aromatic backbone) with related imines^[13] or with a cyclometallated platinum(IV) complex.^[16a,51] In addition to the formation of **8**, a plethora of unidentified side products were observed in the $^{31}\text{P}\{^1\text{H}\}$ NMR spectrum. Previous reports of structurally related complexes with a pyridyl–imine backbone showed the retention of the dimethyliron moiety without evidence for C–C coupling and subsequent degradation upon thermolysis.^[52] The solid-state structure of **9** was established by an X-ray diffraction study of single crystals obtained from *n*-pentane, and the asymmetric unit contains two chemically

equivalent but crystallographically independent molecules (Figure 9).

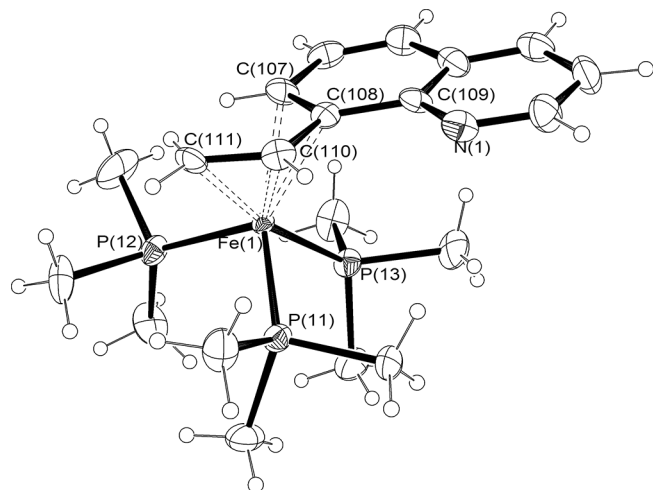


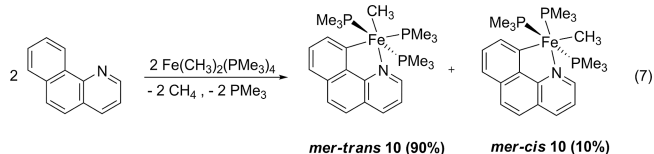
Figure 9. Depiction of the solid-state molecular structure of **9** (only one of crystallographically independent molecule in the asymmetric unit).

In the mononuclear complex **9**, the $\text{Fe}(\text{PMe}_3)_3$ moiety is η^4 -coordinated to the exocyclic C=C group (C111 and C110) and to the aromatic carbon atoms (C108 and C107) of 8-vinylquinoline. The vinylic group lies in the same plane as the aromatic backbone and is bent away from the nitrogen donor group (N1). The bond lengths and angles are as expected and, for example, closely resemble those of the structure obtained by the photolysis of $[(\text{C}_2\text{F}_5)_2\text{PCH}_2\text{CH}_2\text{P}(\text{C}_2\text{F}_5)_2]\text{Fe}(\text{CO})_3$ in the presence of styrene.^[53] If we define the atoms P11, P12, and P13 and the midpoints of the C111–C110 and C102–C108 bonds as the ligand positions, the geometry around the iron center is trigonal bipyramidal. Atoms P11, P12, and the C107–C108 midpoint occupy the equatorial positions, and the PMe_3 group (P13) occupies one of the axial positions. In the other axial position, the C110–C111 midpoint deviates from the ideal trigonal-bipyramidal geometry with a maximum angle of 47.5° , which is due to the fixed geometry of the vinylic group coordinated to the aromatic ring. Thus, the bond lengths and angles are as expected for η^4 -diene coordination for a low-valent iron(0) coordination. Low-valent η^4 -bound monoiron aryl complexes are rare, and a distortion from arene planarity is observed for $[\text{Fe}(\eta^4\text{-C}_{10}\text{H}_8)(\eta^6\text{-C}_6\text{Me}_6)]$ ^[54] and strictly bound aromatic bonds are found in $[\text{K}(18\text{-crown-6})\{\text{Cp}^*\text{Fe}(\eta^4\text{-C}_{10}\text{H}_8)\}]$ (Cp^* = pentamethylcyclopentadienyl) or $[\text{Fe}(\eta^4\text{-C}_{14}\text{H}_{10})\{\text{P}(\text{OMe}_3)_3\}]$.^[55] Interestingly, nitrogen-site-selective η^2 - or η^6 -bound transition-metal coordination within structurally characterized N-heterocyclic aromatic derivatives is rare.^[31,56]

Synthesis of Cyclometalated 7,8-Benzoquinoline

In pursuit of new vinyl-substituted N-heterocyclic benzannulated complexes, we studied the cyclometalation of related 7,8-benzoquinoline with $\text{Fe}(\text{CH}_3)_2(\text{PMe}_3)_4$ [Equa-

tion (7)]. Solutions of $(\kappa^2\text{-C,N-C}_{13}\text{H}_6\text{N})\text{Fe}(\text{CH}_3)(\text{PMe}_3)_3$ (**10**) decompose rapidly in THF at room temperature, but cooled solutions in *n*-pentane are relatively stable. Dark violet crystals from concentrated *n*-pentane solutions were isolated in up to 56% yield. This is remarkable because a similarly conducted reaction with $\text{Co}(\text{CH}_3)(\text{PMe}_3)_4$ failed to form cyclometalated products.



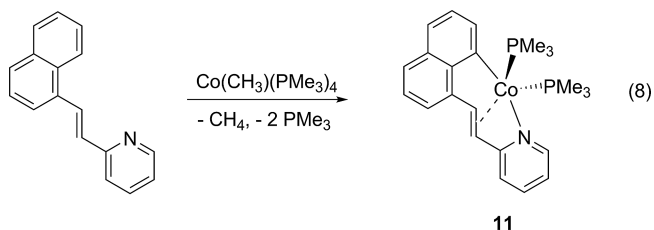
^1H - ^1H NOESY experiments indicated a *mer-trans/cis* configuration across the Fe–P bond, as a cross-peak signal between the Fe–CH₃ group and the methyl protons of the trimethylphosphane ligand was observed. The *mer-trans* to *mer-cis* isomerization of **10** in solution was followed by ^{31}P NMR spectroscopy at room temperature. The *mer-cis/trans* ratio of ca. 1:10 changed after 5 h. Additionally, the process for **10** was more complex as, in addition to *mer-trans* isomerization, a cyclometalated iron(II) hydride byproduct was observed from *cis*- $\text{FeMe}_2(\text{PMe}_3)_2$ followed by reductive C–C coupling (Ar–CH₃) and the release of 10-methyl-7,8-benzoquinoline (NMR spectroscopy) accompanied by the release of transient $\text{Fe}(\text{PMe}_3)_4$, which activates the C–H bond of the quinoline backbone.^[13]

Although the molecular geometry of **10** has not been clarified owing to poor crystal quality, the ^1H NMR signals of the retained Fe–CH₃ group as a singlet at $\delta = -0.58$ ppm and in particular the two sets of triplet/doublet phosphorus resonances for the PMe_3 ligands in the $^{31}\text{P}\{^1\text{H}\}$ NMR spectrum at $\delta = 17.2$ and 27.9 ppm with $^2J_{\text{P,P}} = 38.2$ Hz and at $\delta = 31.3$ and 43.2 ppm with $^2J_{\text{P,P}} = 63.5$ Hz suggest the presence of two isomers with *mer-trans* (90%) and *mer-cis* (10%) configuration, respectively. The structural preferences of six-coordinate diorganyl Fe^{II} complexes have been thoroughly analyzed previously, since 7,8-benzoquinoline is commercially available. The activation of the aryl C–H bond to form five-membered metallacycles has been repeatedly studied in recent years, typically with the fourth- and fifth-row late-transition elements Pd, Pt, Ru, and Ir.^[57,58] It should be noted that a similar reaction of *cis*- $\text{FeMe}_2(\text{PMe}_3)_2$ with a related diphenyl ketimine ($\text{Ph}_2\text{C}=\text{CNH}$) ligand resulted in reductive Ar–CH₃ coupling followed by reinsertion to form a stable Fe–H complex.^[13]

Arylation through CH₄ Loss Accompanied by η^2 -Vinyl Coordination from $\text{Co}(\text{CH}_3)(\text{PMe}_3)_4$

Double C–H bond activation can be envisaged with 2-(2-naphthalene-1-ylvinyl)pyridine and $\text{Co}(\text{CH}_3)(\text{PMe}_3)_4$, as observed previously with $\text{Fe}(\text{CH}_3)_2(\text{PMe}_3)_4$.^[47b,59] For the treatment of $\text{Co}(\text{CH}_3)(\text{PMe}_3)_4$ with the vinylpyridyl ligand [Equation (8)], aryl C–H activation is observed in the first step without consecutive vinylic C–H activation, which can

be attributed to the combined effects of the inertness of the vinylic C–H bond after π -coordination.



From *n*-pentane solutions, dark red rhombic crystals of **11** were obtained. Under argon, decomposition is noticed above 116–119 °C. The IR spectrum contains absorption bands at $\tilde{\nu} = 1581$ and 1565 cm^{-1} [$\nu(\text{C}=\text{C})$] with a bathochromic shift (ca. 70 cm^{-1}) for the vinylic group caused by metalation. The ^1H NMR spectrum (Figure 10) shows the resonances of the two anisochronically oriented trimethylphosphane ligands at $\delta = 1.06$ and 1.25 ppm with $^2J_{\text{P,H}} = 6.9$ and 5.8 Hz , respectively. The π coordination is clarified by two upfield-shifted resonances at $\delta = 3.01$ and 4.68 ppm owing to coordination to the cobalt atom. The aromatic protons resonate in the typical area between $\delta = 6.5$ and 7.7 ppm (Figure 10).

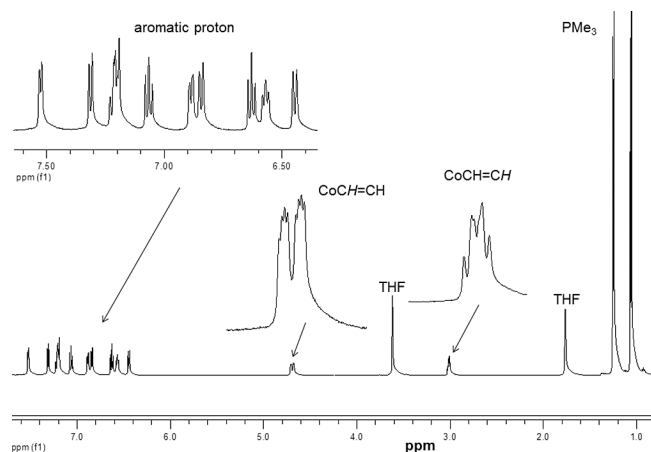


Figure 10. Experimental 500 MHz ^1H NMR spectrum of **11** at 298 K in $[\text{D}_8]\text{THF}$,^[45] showing the upfield-shifted $\text{CoC}(\text{sp}^2)\text{-H}$ resonances.

Notably, we have not observed an upfield-shifted hydride signal in the ^1H NMR spectrum of an in situ experiment with $\text{Co}(\text{CH}_3)(\text{PMe}_3)_4$ and 2-(2-naphthalene-1-ylvinyl)pyridine, as previously observed for an isoelectronic imine ligand (*N*-benzylidene-1-naphthylamine), for which the complex was furthermore structurally characterized as *mer*-($\kappa^3\text{-C,N,C-C}_6\text{H}_4\text{-CH=N-C}_{10}\text{H}_6$) $\text{CoH}(\text{PMe}_3)_3$.^[59] Significantly, the $^{13}\text{C}\{^1\text{H}\}$ NMR spectrum of **11** correspondingly contains two upfield-shifted carbon resonances, which are compatible only with π coordination of the olefin carbon atoms to the cobalt atom. Both carbon atoms of the olefinic function in the aromatic backbone produce doublets owing to coupling with the phosphorus atoms of the two equatorial trimethylphosphane ligands at $\delta = 47.7\text{ ppm}$ with $^2J_{\text{P,C}}$

= 16.3 Hz and at $\delta = 68.8\text{ ppm}$ with $^2J_{\text{P,C}} = 23.8\text{ Hz}$. Similarly to that of **8**, the $^{31}\text{P}\{^1\text{H}\}$ NMR spectrum of **11** at $-70\text{ }^\circ\text{C}$ shows two unresolved resonances as broad singlets at $\delta = 2.52$ and 6.79 ppm , indicating high ligand mobility. Additional attempts at the subsequent thermolysis of **11** led to degradation, and no tractable products of a second vinylic $\text{C}(\text{sp}^2)\text{-H}$ activation could be obtained; hence, these species were not pursued or fully characterized except for routine NMR spectroscopy studies. From *n*-pentane at $-27\text{ }^\circ\text{C}$, a crystal suitable for the characterization of **11** by single-crystal X-ray analysis was obtained. The results of the X-ray studies (ORTEP depiction in Figure 11) showed that the overall geometry around the Co atom in **11** is approximately trigonal bipyramidal ($\tau = 0.89$); the pyridyl and aryl substituents are in the apical positions, and the η^2 -bound alkenyl backbone and two PMe_3 ligands are in the equatorial positions. The bond lengths and angles are in the typical range for previously discussed cobalt–pyridyl complexes (Table 4).

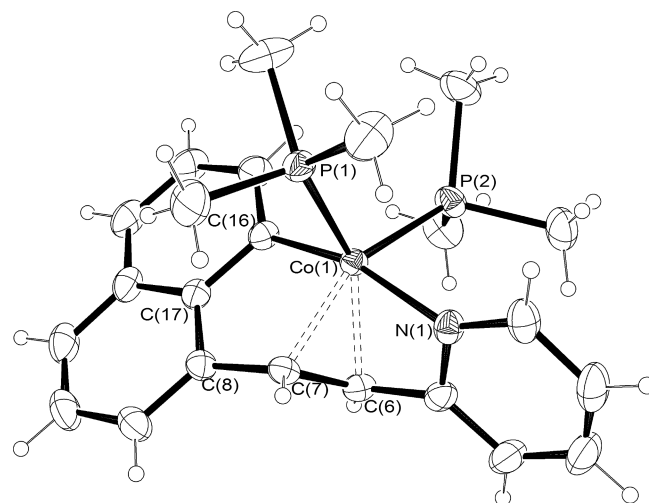


Figure 11. Depiction of the solid-state molecular structure of **11** with 50% probability ellipsoids.

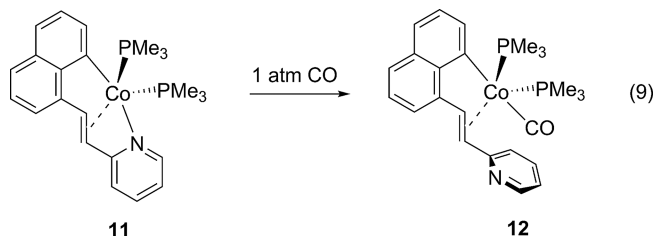
Table 4. Selected bond lengths [\AA] and angles [$^\circ$] of **11** and **12**.

	11	12
$\text{Co-C}(\text{sp}^2)_\sigma$	1.9343(16)	1.9960(15)
$\text{Co-C}(\text{sp}^2)_\pi$	2.0057(16)	2.0608(14)
$\text{Co-C}(\text{sp}^2)_\pi$	2.0043(15)	2.0508(15)
Co-N	2.0540(13)	–
$\text{C}(\text{sp}^2)\text{-C}(\text{sp}^2)_\pi$	1.441(2)	1.431(2)
Co-P_{eq}	2.2314(5)	2.2041(4)
Co-P_{ax}	2.1827(5)	–
$\text{C}(\text{sp}^2)_\sigma\text{-Co-N}$	164.73(6)	–
$\text{C}(\text{sp}^2)_\sigma\text{-Co-}\pi\text{C}(\text{sp}^2)_\pi$	84.60(6)/96.78(6)	86.31(6)/83.45(6)
$\text{P}_{\text{ax}}\text{-Co-P}_{\text{eq}}$	111.05(2)	–
$\text{P}_{\text{eq}}\text{-Co-P}_{\text{eq}}$	–	113.07(2)

Monocarbonyl Substitution by the Release of the Pyridyl N Linkage of **11**

A comparison of the reactivity of **11** with those of the cobalt(I) alkenylpyridine complexes (**1–3**) and a bicyclo-

metalated cobalt(III) imine complex^[59] was achieved by placing solutions of **11** under an atmosphere of carbon monoxide at 20 °C. Although the related Co(III) imine complex is inert against oxidative addition,^[59] carbon monoxide smoothly substitutes the pyridine anchoring group of **11** to form the terminal monocarbonyl complex **12** [Equation (9)]. From *n*-pentane solution, orange needles precipitated in 71% yield, and the crystals start to decompose at 155–157 °C.



From the IR spectrum of **12**, a terminal carbonyl ligand is indicated by a strong absorption band at $\tilde{\nu} = 1954 \text{ cm}^{-1}$. The ^1H , ^{13}C , and $^{31}\text{P}\{^1\text{H}\}$ NMR spectra of **12** show the relationship with the parent complex **11**. The signals of the coordinating alkenyl group are again observed in the up-field area of the ^1H NMR spectrum as doublets of triplets at $\delta = 3.66$ and 5.01 ppm as well as in the corresponding $^{13}\text{C}\{^1\text{H}\}$ NMR spectrum as doublets at $\delta = 60.5$ and 67.9 ppm, which indicates the π -coordination to the metal center. The better electron-donating ability of the pyridyl group causes the terminal carbonyl carbon resonance in the $^{13}\text{C}\{^1\text{H}\}$ NMR spectrum to move to lower field ($\delta = 218.3$ ppm) compared with those of related imine–cobalt complexes. Complex **12** appears stable in the solid state at -27 °C for weeks but readily decomposes in solution at room temperature, as demonstrated by line broadening and the appearance of additional peaks in the NMR spectra. Owing to the high mobility of both asymmetric trimethylphosphane ligands, only a broad multiplet of overlapping signals at $\delta = 12.7$ ppm is observed in the $^{31}\text{P}\{^1\text{H}\}$ NMR spectrum. The overall NMR spectroscopic data confirm this configuration of **12** in solution, and isomers with exchanged carbonyl ligand positions or insertion products are not detected. The retention of alkenyl-bound π -coordination for cobaltocycle **12** was confirmed by elucidation of the molecular structure of crystals grown from concentrated *n*-pentane solution at -27 °C (Figure 12).

The cobalt atom is found in a trigonal-bipyramidal coordination environment ($\tau = 0.96$; Figure 12), as typically found for the majority of pentacoordinate organocobalt(I) complexes.^[60] Two PMe_3 ligands are held in equatorial positions with typical Co–P distances [Co1–P1 2.2040(4) and Co1–P2 2.2180(4) Å]. The third equatorial position is occupied by the olefin carbon atoms with similar bond lengths [Co1–C13 2.0608(14) Å and Co1–C14 2.0508(15) Å]. The bond length between the olefinic carbon atoms [C14–C13 = 1.431(2) Å] is expanded owing to the coordination to the cobalt center and is close to the average value (1.40 Å) for olefin ligands coordinated to a cobalt

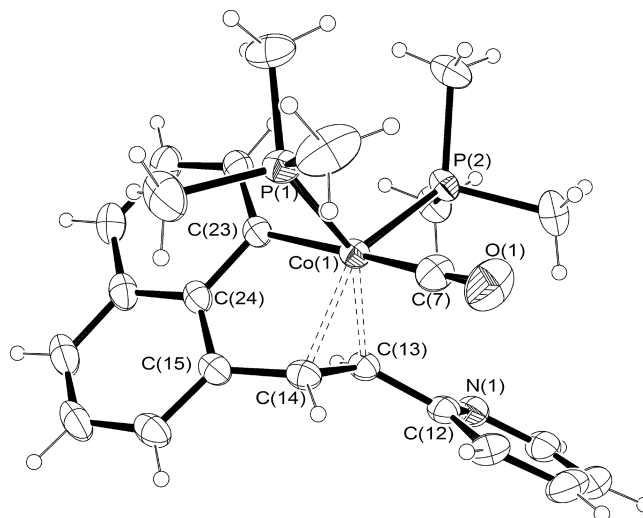
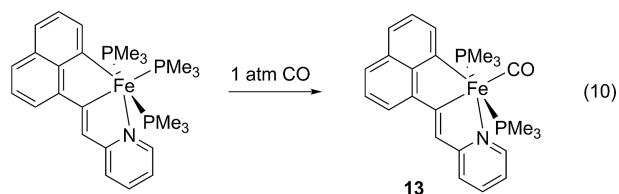


Figure 12. Depiction of the solid-state molecular structure of **12** with 50% probability ellipsoids.

atom. The π coordination is well documented by the high-field shift of the signals of both olefinic carbon atoms (NMR spectroscopy). The carbonyl group and the metalated carbon atom (C23) are orientated in the axial direction [C23–Co1–C7 171.26(7)°]. The bond length between the metalated carbon atom and the cobalt atom [Co1–C23 1.9960(15) Å] is similar to those for the olefinic carbon atoms (C13 and C14). The most-striking structural feature is the release of N coordination, and the pyridyl ring is directed away from the metal center. The olefin coordination in **12** places enough electron density at the metal center to favor carbonyl binding over the binding of the pyridine group. Complex **12** is also a rare example of a complex in which a cobalt atom with oxidation state +1 contains three different types of metal–carbon bonds (Co–C_{Alk}, Co–CH=CH, Co–C≡O).^[31]

Monocarbonyl Substitution versus Release of Pyridyl N Linkage

An experimental distinction of the reactivities of the closely related bicyclic metalated iron–imine complex (κ^3 -C,N,C-C₆H₄-CH=N-C₁₀H₆)Fe(PMe₃)₃^[47b] and pyridyl-cobalt complex **11** was achieved by placing solutions of (κ^3 -C,N,C-C₅H₄N-C=CH-C₁₀H₆)Fe(PMe₃)₃^[47b] under 1 bar of carbon monoxide at 20 °C [Equation (10)]. The retention of the configuration and the regioselective monosubstitution of the trimethylphosphane ligand *trans* to the vinylic carbon atom was observed. A similar reaction pathway is recognized with a series of related iron–imine complexes.^[13] Conversely, with respect to the related reaction pathway of **11** [Equation (9)], we have no evidence for the release of the N-donor linkage of the pyridyl backbone, the insertion of the products into the Fe–C/Fe–N bond,^[61] or multiple substitutions of PMe_3 ligands in the presence of excess carbon monoxide.



The carbonyl complex **13** forms olive green crystals, which can be handled in air for several hours and are thermally stable under argon to 157 °C. It is less soluble in *n*-pentane and diethyl ether and shows moderate solubility in THF. The IR spectrum of **13** display characteristic strong bands at $\tilde{\nu} \approx 1876 \text{ cm}^{-1}$ for a terminal carbonyl ligand and $\tilde{\nu} \approx 1577$ and 1542 cm^{-1} for metalated aromatic C=C groups that experience a slightly hypsochromic shift of ca. 11 cm^{-1} relative to the bands of the parent complex ($\kappa^3\text{-C,C,N-C}_5\text{H}_4\text{N-C=CH-C}_{10}\text{H}_6\text{Fe(PMe}_3\text{)}_3$).^[47b] The $^{31}\text{P}\{^1\text{H}\}$ NMR spectrum shows a singlet at $\delta = 21.1 \text{ ppm}$, which is compatible with two isochronic trimethylphosphane ligands at the *trans* positions of an octahedral coordination sphere and a carbonyl ligand in a *cis* position to produce a *mer-trans* arrangement of the six ligands. The better electron-donating ability of pyridyl group causes the resonance of the terminal carbonyl carbon atom in the $^{13}\text{C}\{^1\text{H}\}$ NMR spectrum to move to lower field ($\delta = 234.3 \text{ ppm}$) compared with that of the isoelectronic iron imine complex ($\kappa^3\text{-C,C,N-C}_6\text{H}_5\text{-CH=N-C}_{10}\text{H}_6\text{Fe(PMe}_3\text{)}_3$ with $\delta = 218.7 \text{ ppm}$ (IR: $\tilde{\nu} = 1883 \text{ cm}^{-1}$).^[47b,59] To date, the bicyclic metalated iron pyridyl complex **13** is the only example in which double C–H activation produces a structure isoelectronic to those obtained with iron–imine complexes.^[47b]

Conclusions

A series of vinyl/aryl organocobalt and iron complexes with pyridyl and pyrazyl ligand backbones were synthesized and characterized. The resultant cobalt and iron complexes are low-spin d^6 and d^8 species. At variance with previous studies of imine ligands, the reverse topology in terms of interchanged 1,4-azadiene ligands showed significant differences in reactivity.^[13] The monocyclometalated cobalt(I) complexes **1–3** readily demetalate from the pyridyl backbone in the presence of carbon monoxide but oxidatively add iodomethane to form stable $\text{CH}_3\text{Co}^{\text{III}}\text{I}$ (**4–6**) metallacycles. Analogous reactions with $\text{Fe}(\text{CH}_3)_2(\text{PMe}_3)_4$ failed to form the related cyclometalated iron 2-alkenylpyridyl complexes. By contrast, bicyclic metalated cobalt complexes with an η^2 -alkenyl coordination motif (**7**, **11**, and **12**) were obtained and simply release their N-donor linkage under 1 atm of carbon monoxide. These differences of the cyclometalation reaction sequence between $\text{Co}(\text{CH}_3)(\text{PMe}_3)_4$ and $\text{Fe}(\text{CH}_3)_2(\text{PMe}_3)_4$ depend upon the nature of the $L_n\text{M}$ fragment ($\text{M} = \text{Co, Fe}$) and suggest that the mechanistic divergence begins with the initial binding of the pyridine nitrogen atom to allow a close approach of the vinylic hydrogen atom to the unsaturated cobalt complex. A reversed competing reaction sequence is observed with 8-vin-

ylquinoline, which lacks a suitable bite angle and favors reductive elimination with the loss of ethane from $\text{Fe}(\text{CH}_3)_2(\text{PMe}_3)_4$ to form **9** with binding solely through the olefinic and aromatic carbon π bonds instead of the combination of η^2 -olefin and *N*-pyridyl coordination observed for the cobalt complex **8**. Investigations of these vinylpyridyl cobalt and iron complexes are of continuing interest in our studies, and further experiments to expand their scope are in progress.

Experimental Section

General Procedures: Unless otherwise stated, all manipulations were performed under an inert atmosphere of nitrogen by using standard Schlenk techniques or an MBraun glovebox. Anhydrous *n*-pentane, toluene, diethyl ether, and THF were purchased from Acros, sparged with nitrogen, and passed through activated alumina. $[\text{D}_6]$ Benzene and $[\text{D}_8]$ THF were dried under reflux with Na/K alloy in sealed vessels under a partial pressure, trap-to-trap distilled, and freeze–pump–thaw degassed three times. $[\text{D}_8]$ Toluene was purified in an analogous manner at reflux over Na. The ^1H , $^{31}\text{P}\{^1\text{H}\}$, and $^{13}\text{C}\{^1\text{H}\}$ spectra were recorded with Bruker DRX and AMX spectrometers operating at 500 and 300 MHz for the proton nuclei. All chemical shifts are reported in parts per million, and all coupling constants are reported in Hertz. The ^1H NMR spectra were referenced to residual solvent protons ($\text{C}_6\text{D}_5\text{H}$, $\delta = 7.16 \text{ ppm}$; $\text{C}_7\text{D}_7\text{H}$, $\delta = 2.09 \text{ ppm}$; $\text{C}_4\text{D}_7\text{HO}$, $\delta = 1.73 \text{ ppm}$) relative to tetramethylsilane at $\delta = 0.00 \text{ ppm}$. The $^{31}\text{P}\{^1\text{H}\}$ NMR spectra were referenced to external 85% H_3PO_4 at $\delta = 0.00 \text{ ppm}$. The $^{13}\text{C}\{^1\text{H}\}$ NMR spectra were referenced to solvent resonances (C_6D_6 , $\delta = 128.0 \text{ ppm}$; C_7D_8 , $\delta = 20.4 \text{ ppm}$; $\text{C}_4\text{D}_8\text{O}$, $\delta = 25.37 \text{ ppm}$). The IR spectra were obtained from Nujol mulls between KBr plates by using a Bruker FRA 106 spectrophotometer and were recorded in the wavenumber range $4000\text{--}400 \text{ cm}^{-1}$. Elemental analyses of air-sensitive substances were performed by H. Kolbe Microanalytical Laboratory, Mülheim an der Ruhr (Germany). The C, H, N analyses of air-stable substances were performed in the microanalysis laboratory of the Clemens-Schöpf-Institut für Organische Chemie und Biochemie at TU-Darmstadt by using a Perkin–Elmer CHN 240 A analyzer. The melting and decomposition points were measured with a Büchi 510 melting point apparatus. Air-sensitive substances were sealed in capillaries under 1 bar of argon. $\text{CoCH}_3(\text{PMe}_3)_4$,^[28a] $\text{Fe}(\text{CH}_3)_2(\text{PMe}_3)_4$,^[62] trimethylphosphane,^[63] tetramethylphosphonium iodide,^[64] and 2-(2-naphthalene-1-ylvinyl)pyridine^[65] were synthesized by literature methods. 2-Vinylpyridine, 2-vinylpyrazine, quinoline-8-carbaldehyde, 7,8-benzoquinoline, 2-benzoylpyridine, and *n*-butyllithium (1.6 M) were purchased from Acros and used as received.

8-Vinylquinoline: At $-70 \text{ }^\circ\text{C}$, a hexane solution of *n*BuLi (33.7 mL, 1.6 N, 53.9 mmol) was slowly added to tetramethylphosphonium iodide (21.8 g, 53.9 mmol) in THF (250 mL). After stirring for 2 h at $20 \text{ }^\circ\text{C}$, the solution was cooled to $-20 \text{ }^\circ\text{C}$, and quinoline-8-carbaldehyde (8.47 g, 53.9 mmol) in THF (50 mL) was added slowly. After warming to ambient temperature, the reaction mixture was heated to reflux for 5 h and quenched with water (250 mL). The THF was removed in vacuo, and the residue was extracted with pentane ($3 \times 100 \text{ mL}$). The organic phases were combined, dried with MgSO_4 , and filtered. The solvent was removed in vacuo, and distillation under reduced pressure afforded 8-vinylquinoline as a colorless oil (isolated yield 9.93 g, 84%); b.p. $121 \text{ }^\circ\text{C}/17 \text{ mbar}$. ^1H

NMR (300 MHz, [D₈]THF, 300 K): δ = 5.48 (dd, $^2J_{\text{H,H}} = 1.3$, $^3J_{\text{H,H}} = 11.1$ Hz, 1 H, C=CH), 6.08 (dd, $^2J_{\text{H,H}} = 1.3$, $^3J_{\text{H,H}} = 17.9$ Hz, 1 H, C=CH), 7.48 (ddd, $^3J_{\text{H,H}} = 8.3$, $^3J_{\text{H,H}} = 5.3$, $^4J_{\text{H,H}} = 1.2$ Hz, 1 H, CH=CH₂), 7.83 (d, $^3J_{\text{H,H}} = 8.1$ Hz, 1 H, Ar-H), 8.02 (d, $^3J_{\text{H,H}} = 7.3$ Hz, 1 H, Ar-H), 8.14 (d, $^3J_{\text{H,H}} = 11.1$ Hz, 1 H, Ar-H), 8.24 (dd, $^3J_{\text{H,H}} = 8.3$, $^4J_{\text{H,H}} = 1.5$ Hz, 1 H, Ar-H), 8.95 (dd, $^4J_{\text{H,H}} = 1.4$, $^3J_{\text{H,H}} = 2.3$ Hz, 1 H, N=CH) ppm. $^{13}\text{C}\{^1\text{H}\}$ NMR (125 MHz, [D₈]THF, 300 K): δ = 115.6 (s, CH₂), 122.2 (s, CH), 125.8 (s, CH), 127.2 (s, CH), 128.6 (s, CH), 129.3 (s, C), 133.9 (s, CH), 136.7 (s, C), 136.9 (s, CH), 146.4 (s, C), 150.5 (s, NCH) ppm. C₁₁H₉N (155.20): calcd. C 85.13, H 5.85, N 9.03; found C 85.01, H 5.72, N 8.90.

2-(1-Phenylvinyl)pyridine: The same procedure as that for 8-vinylquinoline afforded 2-(1-phenylvinyl)pyridine (7.0 g, 38 mmol) as a colorless oil (isolated yield 5.81 g, 84%); b.p. 151 °C/13 mbar. ^1H NMR (300 MHz, [D₈]THF, 300 K): δ = 5.59 (d, $^2J_{\text{H,H}} = 1.6$ Hz, 1 H, C=CH), 6.12 (d, $^2J_{\text{H,H}} = 1.6$ Hz, 1 H, C=CH), 7.20–7.37 (m, 7 H, Ar-H), 7.68 (dt, $^3J_{\text{H,H}} = 11.4$, $^4J_{\text{H,H}} = 1.7$ Hz, 1 H, Ar-H), 8.61 (d, $^3J_{\text{H,H}} = 8.1$ Hz, 1 H, Ar-H) ppm. C₁₃H₁₁N (181.23): calcd. C 86.15, H 6.12, N 7.73; found C 85.99, H 6.03, N 7.61.

[2-(2-Pyridinyl- κ N)ethenyl- κ C]tris(trimethylphosphane)cobalt(I) (1): A solution of 2-vinylpyridine (520 mg, 4.94 mmol) in THF (50 mL) was added to CoMe(PMe₃)₄ (1.87 g, 4.94 mmol) in THF at –78 °C (50 mL). A rapid color change from dark red to green was observed as the mixture warmed. After 5 h, the solvent was removed in vacuo, and the oily residue was extracted with *n*-pentane (2 × 50 mL). Crystallization at 4 °C afforded dark green, rhombic crystals. Isolated yield 910 mg (47%); m.p. 75–77 °C (dec.). IR (Nujol, KBr): $\tilde{\nu}$ = 1581 (m, C=C) cm⁻¹. ^1H NMR (500 MHz, [D₈]THF, 300 K): δ = 1.23 (br s, 27 H, PCH₃), 6.32 (d, $^3J_{\text{H,H}} = 6.6$ Hz, 1 H, C=CH), 6.66 (d, $^3J_{\text{H,H}} = 7.1$ Hz, 1 H, C=CH), 7.02 (br s, 1 H, Ar-H), 7.19 (d, $^4J_{\text{P,H}} = 5.4$ Hz, 1 H, Ar-H), 8.76 (d, $^4J_{\text{P,H}} = 5.1$ Hz, 1 H, NCH), 8.87 (dd, $^3J_{\text{H,H}} = 7.8$, $^3J_{\text{P,H}} = 11.4$ Hz, 1 H, Ar-H) ppm. $^{13}\text{C}\{^1\text{H}\}$ NMR (125 MHz, [D₈]THF, 300 K): δ = 19.5 (d, $^1J_{\text{P,C}} = 16.3$ Hz, PCH₃), 111.5 (s, CH), 119.1 (s, CH), 120.5 (s, CH), 121.7 (s, CH), 147.5 (s, CH), 161.4 (s, C), 189.5 (m, Co–CH) ppm. $^{31}\text{P}\{^1\text{H}\}$ NMR (202 MHz, [D₈]THF, 203 K): δ = 5.8 (br s, 3 P, PCH₃) ppm. C₁₆H₃₃CoNP₃ (391.30): calcd. C 49.11, H 8.50, N 3.58, P 23.75; found C 48.95, H 8.97, N 3.55, P 23.58.

[2-Phenyl-2-(2-pyridinyl- κ N)ethenyl- κ C]tris(trimethylphosphane)cobalt(I) (2): 2-(1-Phenylvinyl)pyridine (380 mg, 2.10 mmol) in diethyl ether (50 mL) at –70 °C was combined with CoMe(PMe₃)₄ (792 mg, 2.10 mmol) in diethyl ether (50 mL). As the mixture warmed, gas evolution (CH₄) was detected; the mixture turned green and was stirred at 20 °C for 16 h. The volatiles were removed in vacuo, and the waxy residue was extracted with pentane (3 × 80 mL). At –27 °C, the solution afforded dark green rhombic crystals of **2**, which were suitable for X-ray diffraction, yield 734 mg (75%); m.p. 101–103 °C (dec.). IR (Nujol, KBr): $\tilde{\nu}$ = 1578 [m, (C=C)], 1157 [m, (Co–CH₃)] cm⁻¹. ^1H NMR (500 MHz, [D₈]THF, 300 K): δ = 1.24 (d, $^2J_{\text{P,H}} = 5.8$ Hz, 27 H, PCH₃), 6.40 (dt, $^3J_{\text{H,H}} = 6.4$, $^4J_{\text{H,H}} = 1.7$ Hz, 1 H, C=C–H), 7.08 (ddd, $^3J_{\text{H,H}} = 7.2$, $^3J_{\text{P,H}} = 5.9$, $^4J_{\text{H,H}} = 1.3$ Hz, 1 H, Ar-H), 7.17–7.23 (m, 3 H, Ar-H), 7.30 (dd, $^3J_{\text{H,H}} = 8.3$, $^4J_{\text{P,H}} = 3.3$, $^4J_{\text{H,H}} = 1.5$ Hz, 1 H, Ar-H), 8.85 (d, $^4J_{\text{P,H}} = 5.3$ Hz, 1 H, Ar-H), 8.87 (q, $^3J_{\text{P,H}} = 12.1$ Hz, 1 H, Co–CH) ppm. $^{13}\text{C}\{^1\text{H}\}$ NMR (125 MHz, [D₈]THF, 300 K): δ = 20.2 (d, $^1J_{\text{P,C}} = 16.9$ Hz, PCH₃), 112.4 (s, CH), 118.8 (s, CH), 121.1 (s, CH), 122.7 (s, CH), 126.5 (s, CH), 127.2 (s, CH), 135.1 (s, CH), 143.2 (s, CH), 148.7 (s, CH), 158.3 (s, CH), 191.2 (m, Co–C) ppm. $^{31}\text{P}\{^1\text{H}\}$ NMR (202 MHz, [D₈]THF, 203 K): δ = 5.6 (br s, 3 P, PCH₃) ppm. C₂₂H₃₇CoNP₃ (467.4): calcd. C 56.53, H 7.98, N 3.00, P 19.88; found C 56.75, H 7.40, N 2.97, P 19.91.

[2-(2-Pyrazyl- κ N)ethenyl- κ C]tris(trimethylphosphane)cobalt(I) (3): 2-Vinylpyridine (207 mg, 1.95 mmol) in THF (50 mL) was combined at –70 °C with CoMe(PMe₃)₄ (740 mg, 1.95 mmol) in THF (50 mL) with the evolution of gas. After 3 h at 20 °C, all volatiles were removed from the mixture in vacuo, and the solid residue was extracted with diethyl ether (80 mL). From the solution, dark green rhombic crystals (350 mg) suitable for X-ray diffraction were obtained. Upon cooling of the solution to –27 °C, a second fraction of **3** was collected and combined with the first, yield 390 mg (51%); m.p. 89–91 °C (dec.). IR (Nujol, KBr): $\tilde{\nu}$ = 1575 [m, (C=C)] cm⁻¹. ^1H NMR (500 MHz, [D₈]THF, 300 K): δ = 1.19 (br s, 27 H, PCH₃), 6.86 (d, $^3J_{\text{H,H}} = 7.3$ Hz, 1 H, C=CH), 7.12 (br s, 1 H, C=CH), 7.19 (d, $^4J_{\text{P,H}} = 5.5$ Hz, 1 H, Ar-H), 8.84 (d, $^4J_{\text{P,H}} = 5.0$ Hz, 1 H, NCH), 9.15 (br s, 1 H, Ar-H) ppm. $^{13}\text{C}\{^1\text{H}\}$ NMR (125 MHz, [D₈]THF, 300 K): δ = 19.2 (d, $^1J_{\text{P,C}} = 15.3$ Hz, PCH₃), 121.7 (s, CH), 145.7 (s, CH), 157.5 (s, CH), 161.4 (s, NC), 192.1 (m, Co=C=CH) ppm. $^{31}\text{P}\{^1\text{H}\}$ NMR (202 MHz, [D₈]THF, 203 K): δ = 4.9 (br s, 3 P, PCH₃) ppm. C₁₅H₃₂CoN₂P₃ (392.3): calcd. C 45.93, H 8.22, N 7.14, P 23.69; found C 46.20, H 7.80, N 7.22, P 24.02.

mer-trans-[2-(2-Pyridinyl- κ N)ethenyl- κ C](iodo)(methyl)bis(trimethylphosphane)cobalt(III) (4): A sample of **1** (620 mg, 1.58 mmol) in *n*-pentane (80 mL) at –70 °C was combined with an excess of iodo-methane (562 mg, 3.96 mmol). After the mixture was stirred for 2 h at 20 °C, a white solid was removed by filtration (PMe₄I). The orange-brown solution was kept at 4 °C and deposited orange-yellow crystals (370 mg) with a cubic shape. The volume of the solution was reduced, and **4** (144 mg) crystallized at –27 °C, yield 514 mg (71%); m.p. 101–103 °C (dec.). IR (Nujol, KBr): $\tilde{\nu}$ = 1576 [w, (C=C)], 1158 [m, (Co–CH₃)] cm⁻¹. ^1H NMR (500 MHz, [D₈]THF, 300 K): δ = 0.48 (t, $^3J_{\text{P,H}} = 9.9$ Hz, 3 H, Co–CH₃), 1.03 (t', $^2J_{\text{P,H}} + ^4J_{\text{P,H}} = 7.7$ Hz, 18 H, PCH₃), 6.73 (dd, $^3J_{\text{H,H}} = 6.4$, $^4J_{\text{H,H}} = 0.5$ Hz, 1 H, Ar-H), 6.78 (dt, $^3J_{\text{H,H}} = 6.5$, $^3J_{\text{P,H}} = 5.1$ Hz, 1 H, Ar-H), 8.14 (br s, 1 H, Ar-H), 8.54 (br s, 1 H, Ar-H), 8.61 (d, $^3J_{\text{H,H}} = 6.9$, $^4J_{\text{H,H}} = 0.5$ Hz, 1 H, Ar-H), 9.74 (br s, 1 H, Ar-H) ppm. $^{13}\text{C}\{^1\text{H}\}$ NMR (125 MHz, [D₈]THF, 300 K): δ = –7.2 (m, Co–CH₃), 12.2 (t', $^1J_{\text{P,C}} + ^3J_{\text{P,C}} = 14.2$ Hz, PCH₃), 119.5 (s, CH), 120.9 (s, CH), 126.2 (s, CH), 148.0 (s, CH), 161.5 (s, C), 184.5 (m, Co–CH) ppm. $^{31}\text{P}\{^1\text{H}\}$ NMR (202 MHz, [D₈]THF, 203 K): δ = 11.6 (br s, 2 P, PCH₃) ppm. C₁₄H₂₇CoINP₂ (457.2): calcd. C 36.78, H 5.95, N 3.06, P 13.55; found C 35.98, H 6.40, N 3.03, P 13.83.

mer-trans-[2-Phenyl-2-(2-pyridinyl- κ N)ethenyl- κ C](iodo)(methyl)bis(trimethylphosphane)cobalt(III) (5): To **2** (890 mg, 1.90 mmol) in *n*-pentane (80 mL) at –70 °C, iodo-methane (594 mg, 4.18 mmol) was added slowly. The dark green mixture was stirred at 20 °C for 2 h under 1 bar of argon. A white solid was removed by filtration through a sintered glass disc (G4), and the resulting orange-brown solution was kept at 4 °C. Orange plate crystals (680 mg) suitable for X-ray diffraction were isolated by decantation, washed with a small amount of cold *n*-pentane, and dried in vacuo, yield 680 mg (67%); m.p. 115–117 °C (dec.). IR (Nujol, KBr): $\tilde{\nu}$ = 1580 [w, (C=C)], 1157 [m, (Co–CH₃)] cm⁻¹. ^1H NMR (500 MHz, [D₈]THF, 300 K): δ = 0.30 (t, $^3J_{\text{P,H}} = 10.0$ Hz, 3 H, Co–CH₃), 0.72 (t', $^2J_{\text{P,H}} + ^4J_{\text{P,H}} = 7.9$ Hz, 18 H, PCH₃), 6.07 (dt, $^3J_{\text{H,H}} = 7.1$, $^4J_{\text{H,H}} = 1.2$ Hz, 1 H, Ar-H), 6.32 (dt, $^3J_{\text{H,H}} = 8.4$, $^4J_{\text{H,H}} = 1.1$ Hz, 1 H, Ar-H), 6.63–6.67 (m, 3 H, Ar-H), 6.85 (ddd, $^3J_{\text{H,H}} = 7.1$, $^4J_{\text{P,H}} = 4.5$, $^4J_{\text{H,H}} = 2.1$ Hz, 1 H, Ar-H), 7.05 (dd, $^3J_{\text{H,H}} = 6.8$, $^4J_{\text{H,H}} = 2.1$ Hz, 1 H, Ar-H), 7.24 (dd, $^3J_{\text{H,H}} = 7.1$, $^4J_{\text{H,H}} = 1.5$ Hz, 1 H, Ar-H), 8.53 (t, $^3J_{\text{H,H}} = 6.8$, $^4J_{\text{P,H}} = 4.6$ Hz, 1 H, Ar-H) ppm. $^{13}\text{C}\{^1\text{H}\}$ NMR (125 MHz, [D₈]THF, 300 K): δ = –7.4 (m, Co–CH₃), 8.52 (t', $^1J_{\text{P,C}} + ^3J_{\text{P,C}} = 12.9$ Hz, PCH₃), 110.1 (s, CH), 113.5 (s, CH), 118.8 (s, CH), 120.1 (s, CH), 123.6 (s, CH), 125.8 (s, CH), 128.6 (s, CH), 137.9 (s, CH), 149.3 (s, C), 183.5 (m, Co–C) ppm. $^{31}\text{P}\{^1\text{H}\}$ NMR (202 MHz, [D₈]THF, 203 K): δ = 8.9 (br s, 2 P, PCH₃) ppm.

$C_{20}H_{31}CoINP_2$ (533.3): calcd. C 45.05, H 5.86, N 2.63, P 11.62; found C 45.11, H 6.38, N 2.67, P 11.86.

mer-trans-[2-(2-Pyrazyl- κ N)ethenyl- κ C](iodo)(methyl)bis(trimethylphosphane)cobalt(III) (6): A sample of **3** (560 mg, 1.42 mmol) in THF (50 mL) at -70°C was combined with iodomethane (445 mg, 3.14 mmol). After 16 h at 20°C , an off-white solid, tetramethylphosphonium iodide (IR spectroscopy), was removed by filtration, and the filtrate was evaporated to dryness. Extraction with diethyl ether (3×60 mL) and cooling to -27°C afforded orange-brown crystals of **6**, which were suitable for X-ray diffraction, yield 398 mg (61%); m.p. $103\text{--}106^\circ\text{C}$ (dec.). IR (Nujol, KBr): $\tilde{\nu} = 1579$ [m, (C=C)], 1162 [w, (Co-CH₃)] cm^{-1} . ^1H NMR (500 MHz, [D₈]THF, 300 K): $\delta = 0.45$ (t, $^3J_{\text{P,H}} = 8.5$ Hz, 3 H, Co-CH₃), 0.98 (t', $^2J_{\text{P,H}} + ^4J_{\text{P,H}} = 7.6$ Hz, 18 H, PCH₃), 6.75 (t, $^3J_{\text{H,H}} = 6.4$ Hz, 1 H, Ar-H), 6.78 (dt, $^3J_{\text{H,H}} = 6.5$, $^3J_{\text{P,H}} = 5.1$ Hz, 1 H, Ar-H), 8.21 (br s, 1 H, Ar-H), 8.52 (br s, 1 H, Ar-H), 8.75 (br s, 1 H, Ar-H), 9.80 (br s, 1 H, Ar-H) ppm. $^{13}\text{C}\{^1\text{H}\}$ NMR (125 MHz, [D₈]THF, 300 K): $\delta = -6.5$ (m, Co-CH₃), 12.2 (t', $^1J_{\text{P,C}} + ^3J_{\text{P,C}} = 14.5$ Hz, PCH₃), 125.0 (s, CH), 148.0 (s, CH), 144.2 (s, CH), 157.1 (s, CH), 162.5 (s, C), 183.9 (m, Co-CH) ppm. $^{31}\text{P}\{^1\text{H}\}$ NMR (202 MHz, [D₈]THF, 203 K): $\delta = 10.5$ (br s, 2 P, PCH₃) ppm. $C_{13}H_{26}CoIN_2P_2$ (458.2): calcd. C 34.08, H 5.72, N 6.11, P 13.52; found C 33.76, H 6.03, N 5.88, P 13.43.

[2-(1-Phenyl- η^2 -ethenyl)pyridine][2-phenyl-2-(2-pyridyl- κ N)ethenyl- κ C](trimethylphosphane)cobalt(I) (7): A solution of $\text{CoMe}(\text{PMe}_3)_4$ (742 mg, 1.96 mmol) in THF (70 mL) was combined at -70°C with 2-(1-phenylvinyl)pyridine (711 mg, 3.92 mmol) in THF (50 mL), and a gas evolved. The reaction mixture turned from orange-red to green and finally to brown. After 16 h at 20°C , all volatiles were removed from the mixture in vacuo, and the solid residue was extracted with *n*-pentane (2×80 mL). From the solution, dark brown cubic crystals (357 mg) suitable for X-ray diffraction were obtained. Upon cooling to -27°C , a second fraction of **7** was collected and combined with the first, yield 808 mg (83%); m.p. $142\text{--}144^\circ\text{C}$ (dec.). IR (Nujol, KBr): $\tilde{\nu} = 1579$ [m, (C=C)] cm^{-1} . ^1H NMR (500 MHz, [D₈]THF, 300 K): $\delta = 1.21$ (d, $^2J_{\text{P,H}} = 7.7$ Hz, 9 H, PCH₃), 2.60 (s, 1 H, C=CH), 2.64 (d, $^3J_{\text{P,H}} = 14.1$ Hz, 1 H, C=CH), 6.57 (dd, $^3J_{\text{H,H}} = 8.1$, $^4J_{\text{H,H}} = 0.5$ Hz, 1 H, C=CH), $6.64\text{--}6.67$ (m, 3 H, Ar-H), $6.85\text{--}6.87$ (m, 4 H, Ar-H), 6.97 (t, $^3J_{\text{H,H}} = 7.3$ Hz, 1 H, Ar-H), 7.01 (t, $^3J_{\text{H,H}} = 7.3$ Hz, 1 H, Ar-H), 7.19 (d, $^3J_{\text{H,H}} = 7.1$ Hz, 1 H, Ar-H), 7.28 (dt, $^3J_{\text{H,H}} = 8.0$, $^3J_{\text{H,H}} = 1.5$ Hz, 1 H, Ar-H), 7.31 (d, $^3J_{\text{P,H}} = 3.1$ Hz, 1 H, CoCH), 7.36 (dd, $^3J_{\text{H,H}} = 8.0$, $^4J_{\text{H,H}} = 0.8$ Hz, 1 H, Ar-H), 7.38 (m, 1 H, Ar-H), 8.07 (d, $^4J_{\text{P,H}} = 5.0$ Hz, 1 H, NCH) ppm. $^{13}\text{C}\{^1\text{H}\}$ NMR (125 MHz, [D₈]THF, 300 K): $\delta = 15.9$ (d, $^1J_{\text{P,C}} = 18.8$ Hz, PCH₃), 38.1 (s, CH₂), 60.5 (d, $^2J_{\text{P,C}} = 11.3$ Hz, C=CH₂), 112.1 (d, $^5J_{\text{P,C}} = 3.8$ Hz, CH), 116.4 (d, $^2J_{\text{P,C}} = 47.5$ Hz, CH), 118.7 (s, CH), 123.1 (s, CH), 124.9 (s, CH), 126.7 (d, $^6J_{\text{P,C}} = 2.5$ Hz, CH), 127.8 (d, $^3J_{\text{P,C}} = 32.5$ Hz, CH), 128.4 (s, CH), 130.8 (s, CH), 136.2 (s, CH), 142.0 (d, $^3J_{\text{P,C}} = 8.8$ Hz, C), 144.1 (d, $^6J_{\text{P,C}} = 3.8$ Hz, C), 148.4 (s, CH), 150.8 (s, CH), 163.9 (s, C), 165.8 (d, $^5J_{\text{P,C}} = 6.3$ Hz, C), 199.5 (m, Co-CH) ppm. $^{31}\text{P}\{^1\text{H}\}$ NMR (202 MHz, [D₈]THF, 203 K): $\delta = 13.6$ (s, 1 P, PCH₃) ppm. $C_{29}H_{30}CoN_2P$ (496.5): calcd. C 70.16, H 6.09, N 5.64, P 6.24; found C 69.78, H 5.72, N 5.69, P 6.35.

[(8-Quinolinyln- κ N)ethenyl- η^2 - κ C,C](methyl)bis(trimethylphosphane)cobalt(I) (8): 8-Vinylquinoline (520 mg, 3.35 mmol) in THF (30 mL) was combined at -80°C with $\text{CoMe}(\text{PMe}_3)_4$ (1.26 g, 3.35 mmol) in THF (50 mL). The mixture turned from red to dark violet-blue as it warmed and was then kept at 20°C for 16 h. The volatiles were removed in vacuo, and the solid residue was extracted with *n*-pentane (3×70 mL). The solution was cooled to -27°C to afford dark violet needles of **8**, which were suitable for X-ray

diffraction. Isolated yield: 940 mg (74%); m.p. $120\text{--}124^\circ\text{C}$ (dec.). IR (Nujol, KBr): $\tilde{\nu} = 1586$ (m), 1568 [w, (C=C)], 1169 (w), 1142 [w, (Co-CH₃)] cm^{-1} . ^1H NMR (500 MHz, [D₈]THF, 300 K): $\delta = -1.77$ (apparent t, $^3J_{\text{P,H}} = 7.2$ Hz, 3 H, Co-CH₃), 0.86 (d, $^2J_{\text{P,H}} = 4.8$ Hz, 9 H, PCH₃), 1.40 (d, $^2J_{\text{P,H}} = 4.2$ Hz, 9 H, PCH₃), 1.93 (d, $^2J_{\text{P,H}} = 7.9$ Hz, 1 H, C=CH), 2.02 (dd, $^3J_{\text{H,H}} = 7.4$, $^3J_{\text{P,H}} = 5.3$ Hz, 1 H, C=CH), 2.64 (t, $^3J_{\text{H,H}} = 8.1$ Hz, 1 H, C=CH), 6.83 (dd, $^4J_{\text{P,H}} = 4.9$, $^3J_{\text{H,H}} = 8.1$ Hz, 1 H, Ar-H), $7.04\text{--}7.08$ (m, 3 H, Ar-H), 7.31 (dd, $^4J_{\text{P,H}} = 4.5$, $^3J_{\text{H,H}} = 8.3$ Hz, 1 H, Ar-H), 8.39 (d, $^4J_{\text{P,H}} = 4.9$ Hz, 1 H, NCH) ppm. $^{13}\text{C}\{^1\text{H}\}$ NMR (125 MHz, [D₈]THF, 300 K): $\delta = -14.5$ (apparent t, $^2J_{\text{P,C}} = 12.7$ Hz, CoCH₃), 15.2 (d, $^1J_{\text{P,C}} = 10.7$ Hz, PCH₃), 16.8 (d, $^1J_{\text{P,C}} = 11.7$ Hz, PCH₃), 49.7 (d, $^2J_{\text{P,C}} = 16.7$ Hz, CH=CH₂), 53.8 (d, $^2J_{\text{P,C}} = 16.4$ Hz, CH=CH₂), 117.8 (s, CH), 119.0 (s, CH), 120.1 (s, CH), 125.8 (s, CH), 127.9 (s, C), 130.8 (s, CH), 151.5 (dd, $^4J_{\text{P,C}} = 4.4$, $^4J_{\text{P,C}} = 4.2$ Hz, NCH), 156.3 (s, C) ppm. $^{31}\text{P}\{^1\text{H}\}$ NMR (202 MHz, [D₈]THF, 203 K): $\delta = 13.6$ (d, $^2J_{\text{P,P}} = 61.3$ Hz, 1 P, PCH₃), 16.8 (d, $^2J_{\text{P,P}} = 61.3$ Hz, 1 P, PCH₃) ppm. $C_{18}H_{30}CoNP_2$ (381.2): calcd. C 56.70, H 7.99, N 3.67, P 16.25; found C 56.85, H 7.68, N 3.68, P 16.29.

[(8-Quinolinyln- η^2 - κ C,C)ethenyl- η^2 - κ C,C]tris(trimethylphosphane)iron(0) (9): $\text{FeMe}_2(\text{PMe}_3)_4$ (1.08 g, 2.77 mmol) in *n*-pentane (30 mL) was combined with 8-vinylquinoline (430 mg, 2.77 mmol) in *n*-pentane (50 mL) at -70°C . Gas evolution was detected as the mixture warmed, and the mixture turned from orange-brown to dark brown when it was kept at 20°C for 10 min. The volatiles were then removed in vacuo, and the waxy residue was extracted with *n*-pentane (2×50 mL). The solution was cooled to 4°C to afford dark red-brown crystals of **9**, which were suitable for X-ray diffraction, yield 474 mg (39%); m.p. $115\text{--}119^\circ\text{C}$ (dec.). IR (Nujol, KBr): $\tilde{\nu} = 1572$ (m), 1533 [m, (v C=C)], 933 [s, ρ_1 (PCH₃)] cm^{-1} . Magnetic moment: $\mu_{\text{eff}} = 1.98 \mu_{\text{B}}$. $C_{20}H_{30}FeNP_3$ (439.3): calcd. C 54.68, H 8.26, N 3.19; found C 54.38, H 7.62, N 3.25.

mer-trans-Methyl[(benzo[h]quinoline-10-yl)- κ C, κ N]tris(trimethylphosphane)iron(II) (10): 7,8-Benzoquinoline (377 mg, 1.85 mmol) in THF (30 mL) was combined with $\text{FeMe}_2(\text{PMe}_3)_4$ (729 mg, 1.85 mmol) in THF (80 mL) at -70°C . As the mixture warmed, it became violet-brown, and the evolution of gas was observed. The mixture was kept at 20°C for 5 h. The volatiles were removed in vacuo, and the solid residue was extracted with diethyl ether (2×70 mL); the solution was cooled to -27°C to afford brown-violet crystals of **10**. Isolated yield 566 mg (64%); m.p. $82\text{--}84^\circ\text{C}$ (dec.). IR (Nujol, KBr): $\tilde{\nu} = 1577$ (m), 1538 [m, (v C=C)], 937 [s, ρ_1 (PCH₃)] cm^{-1} . ^1H NMR (500 MHz, [D₈]THF, 300 K): $\delta = -0.58$ (s, 3 H, Fe-CH₃), 0.47 (br s, 18 H, PCH₃), 0.95 (br s, 9 H, PCH₃), 6.70 (m, 1 H, Ar-H), 6.87 (m, 1 H, Ar-H), 7.04 (m, 1 H, Ar-H), $7.19\text{--}7.24$ (m, 3 H, Ar-H), 8.70 (m, 1 H, Ar-H), 9.16 (m, 1 H, Ar-H) ppm. $^{13}\text{C}\{^1\text{H}\}$ NMR (125 MHz, [D₈]THF, 300 K): $\delta = -18.6$ (m, Fe-CH₃), 14.7 (s, PCH₃), 20.1 (d, $^1J_{\text{P,C}} = 12.5$ Hz, PCH₃), 20.5 (d, $^1J_{\text{P,C}} = 16.3$ Hz, PCH₃), 115.3 (s, CH), 117.8 (s, CH), 121.5 (s, CH), 124.4 (s, CH), 126.8 (s, CH), 127.5 (s, CH), 129.7 (s, CH), 134.3 (s, CH), 139.1 (s, CH), 141.2 (s, C), 151.1 (s, C), 159.3 (s, C), 191.1 (s, Fe-C) ppm. $^{31}\text{P}\{^1\text{H}\}$ NMR (202 MHz, [D₈]THF, 203 K): *cis* (10%): $\delta = 31.3$ (d, $^2J_{\text{P,P}} = 63.5$ Hz, 2 P, PCH₃), 43.2 (t, $^2J_{\text{P,P}} = 63.5$ Hz, 1 P, PCH₃); *trans* (90%): $\delta = 17.2$ (t, $^2J_{\text{P,P}} = 38.2$ Hz, 1 P, PCH₃), 27.9 (d, $^2J_{\text{P,P}} = 38.2$ Hz, 2 P, PCH₃) ppm. $C_{23}H_{38}FeNP_3$ (477.3): calcd. C 57.87, H 8.02, N 2.93, P 19.47; found C 57.43, H 7.91, N 2.97, P 19.71.

{(1,8-Naphthalenediyl- κ C)}[(2-pyridinyl- κ N)ethenylidene- η^2 - κ C,C]bis(trimethylphosphane)cobalt(I) (11): 2-(2-Naphthalene-1-ylvinyl)pyridine (750 mg, 3.24 mmol) in diethyl ether (50 mL) was combined with $\text{CoMe}(\text{PMe}_3)_4$ (1.22 g, 3.24 mmol) in diethyl ether (50 mL) at -70°C with the evolution of gas. After 16 h at 20°C ,

all volatiles were removed from the mixture in vacuo, and the solid residue was washed with cold *n*-pentane to afford **11** as red powder. From a concentrated *n*-pentane solution at 4 °C, dark red rhombic crystals suitable for X-ray diffraction were obtained, yield 1.23 g (87%); m.p. 116–119 °C (dec.). IR (Nujol, KBr): $\tilde{\nu}$ = 1581 (w), 1565 [m, (C=C)] cm^{-1} . ^1H NMR (500 MHz, $[\text{D}_8]\text{THF}$, 300 K): δ = 1.06 (d, $^2J_{\text{P,H}} = 6.9$ Hz, 9 H, PCH_3), 1.25 (d, $^2J_{\text{P,H}} = 5.8$ Hz, 9 H, PCH_3), 3.01 (ddd, $^3J_{\text{P,H}} = 4.5$, $^3J_{\text{P,H}} = 6.8$, $^3J_{\text{H,H}} = 14.1$ Hz, 1 H, C=CH),

4.68 (ddd, $^3J_{\text{P,H}} = 4.5$, $^3J_{\text{P,H}} = 6.8$, $^3J_{\text{H,H}} = 14.1$ Hz, 1 H, C=CH), 6.43 (d, $^3J_{\text{H,H}} = 7.8$ Hz, 1 H, Ar-H), 6.55 (t, $^3J_{\text{H,H}} = 6.8$ Hz, 1 H, Ar-H), 6.64 (d, $^3J_{\text{H,H}} = 7.4$ Hz, 1 H, Ar-H), 6.83 (d, $^3J_{\text{H,H}} = 6.0$ Hz, 1 H, Ar-H), 6.87 (d, $^3J_{\text{H,H}} = 7.0$ Hz, 1 H, Ar-H), 7.06 (d, $^3J_{\text{H,H}} = 7.2$ Hz, 1 H, Ar-H), 7.17–7.21 (m, 2 H, Ar-H), 7.31 (d, $^3J_{\text{H,H}} = 6.8$ Hz, 1 H, Ar-H), 7.52 (d, $^3J_{\text{H,H}} = 4.8$ Hz, 1 H, NCH) ppm. $^{13}\text{C}\{^1\text{H}\}$ NMR (125 MHz, $[\text{D}_8]\text{THF}$, 300 K): δ = 15.3 (d, $^1J_{\text{P,C}} = 17.5$ Hz, PCH_3), 17.1 (d, $^1J_{\text{P,C}} = 13.7$ Hz, PCH_3), 47.7 (d, $^2J_{\text{P,C}} =$

Table 5. Data and structure refinement parameters for **2**, **3**, **5–9**, **11**, and **12**.

	2	3	5	6	7
Empirical formula	$\text{C}_{22}\text{H}_{37}\text{CoNP}_3$	$\text{C}_{15}\text{H}_{32}\text{CoN}_2\text{P}_3$	$\text{C}_{20}\text{H}_{31}\text{CoINP}_2$	$\text{C}_{13}\text{H}_{26}\text{CoIN}_2\text{P}_2$	$\text{C}_{29}\text{H}_{30}\text{CoN}_2\text{P}$
Molecular mass	467.4	392.3	533.2	458.1	496.5
Crystal size [mm]	$0.50 \times 0.30 \times 0.25$	$0.40 \times 0.38 \times 0.30$	$0.50 \times 0.40 \times 0.35$	$0.50 \times 0.20 \times 0.20$	$0.30 \times 0.30 \times 0.25$
Crystal system	monoclinic	triclinic	monoclinic	monoclinic	orthorhombic
Space group	$P2_1/n$	$P\bar{1}$	$P2_1/c$	$P2_1/n$	$P2_12_12_1$
<i>a</i> [Å]	9.0903(5)	8.8552(6)	9.8825(5)	8.8325(6)	8.8673(7)
<i>b</i> [Å]	23.4947(12)	9.8628(7)	15.6644(9)	13.1611(9)	10.2926(8)
<i>c</i> [Å]	12.5417(6)	13.0630(9)	17.3539(10)	16.082(1)	27.879(2)
α [°]	90	84.506(1)	90	90	90
β [°]	101.303(1)	76.085(1)	94.550(1)	96.287(1)	90
γ [°]	90	64.835(1)	90	90	90
<i>V</i> [Å ³]	2512.2(2)	1002.27(12)	2678.0(3)	1858.2(2)	2544.4(3)
<i>Z</i>	4	2	4	4	4
<i>D</i> _{calcd.} [g/cm ³]	1.236	1.300	1.323	1.638	1.296
$\mu(\text{Mo-K}\alpha)$ [mm ⁻¹]	0.881	1.092	1.916	2.748	0.756
Temperature [K]	293(2)	293(2)	293(2)	293(2)	298(2)
Data coll. [°]	$3.5 \leq 2\theta \leq 56$	$3.2 \leq 2\theta \leq 56$	$3.5 \leq 2\theta \leq 56$	$4.0 \leq 2\theta \leq 56$	$4.2 \leq 2\theta \leq 52$
<i>h</i>	$-12 \leq h \leq 12$	$-11 \leq h \leq 11$	$-13 \leq h \leq 13$	$-11 \leq h \leq 11$	$-11 \leq h \leq 10$
<i>k</i>	$-31 \leq k \leq 31$	$-13 \leq k \leq 6$	$-20 \leq k \leq 20$	$-17 \leq k \leq 12$	$-12 \leq k \leq 12$
<i>l</i>	$-16 \leq l \leq 16$	$-15 \leq l \leq 17$	$-23 \leq l \leq 23$	$-21 \leq l \leq 21$	$-34 \leq l \leq 34$
Absorption correction	semiempirical	semiempirical	semiempirical	semiempirical	semiempirical
Reflections measured	29088	6459	36777	11582	16901
Unique data	6025 ($R_{\text{int}} = 0.0362$)	4480 ($R_{\text{int}} = 0.0121$)	6658 ($R_{\text{int}} = 0.0228$)	4342 ($R_{\text{int}} = 0.033$)	5187 ($R_{\text{int}} = 0.043$)
Parameters	253	200	234	172	308
GoF on <i>F</i> ²	1.014	1.035	1.169	0.912	1.064
<i>R</i> 1 [$I \geq 2\sigma(I)$]	0.0321	0.0303	0.0448	0.0344	0.0386
<i>wR</i> 2 (all data)	0.0930	0.0827	0.1683	0.0734	0.0922
	8	9	11	12	
Empirical formula	$\text{C}_{18}\text{H}_{30}\text{CoNP}_2$	$\text{C}_{20}\text{H}_{36}\text{FeNP}_3$	$\text{C}_{23}\text{H}_{30}\text{CoNP}_2$	$\text{C}_{24}\text{H}_{30}\text{CoNOP}_2$	
Molecular mass	381.3	439.3	441.3	469.36	
Crystal size [mm]	$0.50 \times 0.20 \times 0.05$	$0.40 \times 0.20 \times 0.06$	$0.40 \times 0.20 \times 0.06$	$0.50 \times 0.40 \times 0.35$	
Crystal system	triclinic	monoclinic	monoclinic	monoclinic	
Space group	$P\bar{1}$	$P2_1/c$	$P2_1/c$	$P2_1/c$	
<i>a</i> [Å]	7.3529(7)	18.3525(16)	9.2353(3)	8.3930(4)	
<i>b</i> [Å]	10.8500(11)	15.4249(14)	15.8948(6)	14.2682(7)	
<i>c</i> [Å]	13.4218(14)	16.5084(14)	15.5438(6)	19.6087(9)	
α [°]	79.522(2)	90	90	90	
β [°]	79.235(2)	103.068(2)	102.193(1)	90.572(1)	
γ [°]	73.633(2)	90	90	90	
<i>V</i> [Å ³]	999.78(17)	4552.3(7)	2230.3(1)	2348.08(19)	
<i>Z</i>	2	8	4	4	
<i>D</i> _{calcd.} [g/cm ³]	1.267	1.282	1.314	1.328	
$\mu(\text{Mo-K}\alpha)$ [mm ⁻¹]	1.015	0.877	0.921	0.882	
Temperature [K]	293(2)	298(2)	298(2)	298(2)	
Data coll. [°]	$3.0 \leq 2\theta \leq 54$	$2.3 \leq 2\theta \leq 56$	$3.7 \leq 2\theta \leq 56$	$3.5 \leq 2\theta \leq 56$	
<i>h</i>	$-9 \leq h \leq 9$	$-24 \leq h \leq 22$	$-12 \leq h \leq 12$	$-11 \leq h \leq 11$	
<i>k</i>	$-13 \leq k \leq 13$	$-20 \leq k \leq 20$	$-21 \leq k \leq 21$	$-19 \leq k \leq 19$	
<i>l</i>	$-17 \leq l \leq 17$	$-22 \leq l \leq 22$	$-20 \leq l \leq 20$	$-26 \leq l \leq 26$	
Absorption correction	semiempirical	semiempirical	semiempirical	semiempirical	
Reflections measured	11177	57200	30443	31948	
Unique data	4352 ($R_{\text{int}} = 0.022$)	11345 ($R_{\text{int}} = 0.109$)	5551 ($R_{\text{int}} = 0.027$)	5824 ($R_{\text{int}} = 0.019$)	
Parameters	206	470	250	268	
GoF on <i>F</i> ²	1.045	1.091	1.045	1.039	
<i>R</i> 1 [$I \geq 2\sigma(I)$]	0.0329	0.1185	0.031	0.0313	
<i>wR</i> 2 (all data)	0.0922	0.4017	0.084	0.0865	

16.3 Hz, C=CH), 68.8 (d, $^2J_{PC} = 23.8$ Hz, C=CH), 109.4 (d, $^3J_{PC} = 5.0$ Hz, CH), 115.9 (s, CH), 116.5 (s, CH), 117.8 (d, $^3J_{PC} = 5.0$ Hz, CH), 121.8 (s, CH), 122.3 (s, CH), 122.7 (s, CH), 130.8 (s, C), 133.7 (s, CH), 134.6 (dd, $^3J_{PC} = 11.3$, $^3J_{PC} = 5.0$ Hz, CH), 147.7 (d, $^3J_{PC} = 6.3$ Hz, C), 149.8 (s, C), 151.2 (s, CH), 163.3 (m, Co-C), 166.7 (s, NC) ppm. $^{31}\text{P}\{^1\text{H}\}$ NMR (202 MHz, $[\text{D}_8]\text{THF}$, 296 K): $\delta = 2.52$ (br s, 1 P, PCH_3), 6.79 (br s, 1 P, PCH_3) ppm. $\text{C}_{23}\text{H}_{30}\text{CoNP}_2$ (441.4): calcd. C 62.59, H 6.85, N 3.17, P 14.04; found C 62.65, H 6.63, N 3.20, P 14.13.

[(1,8-Naphthalenediyl- κC)(2-pyridine)ethenylidene- $\eta^2\text{-}\kappa\text{C}$, Cl](carbonyl)bis(trimethylphosphane)cobalt(I) (12): A sample of **11** (470 mg, 1.06 mmol) in diethyl ether (70 mL) was stirred under 1 bar of carbon monoxide for 30 min at 20 °C to form a light yellow precipitate. The volatiles were removed in vacuo, and the solid residue was extracted with *n*-pentane (2 × 70 mL). A concentrated solution at -27 °C afforded orange crystals of **12**, yield 354 mg (71%); m.p. 155–157 °C (dec.). IR (Nujol, KBr): $\tilde{\nu} = 1954$ [vs, (C=O)], 1584 (m), 1556 [w, (C=C)] cm^{-1} . ^1H NMR (500 MHz, $[\text{D}_8]\text{THF}$, 296 K): $\delta = 0.83$ (d, $^2J_{PH} = 8.5$ Hz, 9 H, PCH_3), 1.39 (d, $^2J_{PH} = 7.7$ Hz, 9 H, PCH_3), 3.66 (ddd, $^3J_{PH} = 5.6$, $^3J_{HH} = 7.2$, $^4J_{HH} = 2.0$ Hz, 1 H, C=CH), 5.01 (dt, $^3J_{PH} = 5.5$, $^3J_{HH} = 9.4$ Hz, 1 H, C=CH), 6.78 (ddd, $^3J_{HH} = 6.1$, $^4J_{HH} = 1.4$, $^4J_{HH} = 1.0$ Hz, 1 H, Ar-H), 6.96 (dd, $^3J_{HH} = 7.2$, $^3J_{HH} = 7.7$ Hz, 2 H, Ar-H), 7.17 (dd, $^3J_{HH} = 7.8$, $^3J_{HH} = 7.0$ Hz, 1 H, Ar-H), 7.13 (m, 2 H, Ar-H), 7.21 (d, $^3J_{HH} = 6.3$ Hz, 1 H, Ar-H), 7.25 (d, $^3J_{HH} = 8.0$ Hz, 1 H, Ar-H), 7.36 (dt, $^3J_{HH} = 7.7$, $^4J_{HH} = 2.0$ Hz, 1 H, Ar-H), 8.26 (td, $^4J_{HH} = 0.8$, $^4J_{PH} = 4.8$ Hz, 1 H, NCH) ppm. $^{13}\text{C}\{^1\text{H}\}$ NMR (125 MHz, $[\text{D}_8]\text{THF}$, 300 K): $\delta = 16.9$ (d, $^1J_{PC} = 23.9$ Hz, PCH_3), 17.2 (d, $^1J_{PC} = 21.5$ Hz, PCH_3), 60.5 (d, $^2J_{PC} = 12.9$ Hz, C=CH), 67.9 (d, $^2J_{PC} = 9.8$ Hz, C=CH), 116.7 (s, CH), 117.3 (s, CH), 117.5 (s, CH), 119.2 (s, CH), 122.3 (s, CH), 123.4 (s, CH), 123.7 (s, CH), 132.9 (d, $^2J_{PC} = 10.9$ Hz, C), 133.1 (d, $^3J_{PC} = 6.1$ Hz, CH), 133.8 (s, CH), 143.8 (s, C), 147.7 (s, CH), 152.0 (s, C), 165.9 (s, NC), 170.1 (m, Co-C), 218.3 (m, Co-CO) ppm. $^{31}\text{P}\{^1\text{H}\}$ NMR (202 MHz, $[\text{D}_8]\text{THF}$, 296 K): $\delta = 12.7$ (br m, 2 P, PCH_3) ppm. $\text{C}_{24}\text{H}_{30}\text{CoNOP}_2$ (469.4): calcd. C 61.41, H 6.44, N 2.98, P 13.20; found C 61.09, H 6.10, N 2.93, P 13.54.

[(1,8-Naphthalenediyl- κC)(2-pyridinyl- κN)ethenylidene- κC](carbonyl)bis(trimethylphosphane)iron(II) (13): A sample of $[(\kappa^3\text{-C}_6\text{H}_4\text{-CH=N-C}_{10}\text{H}_6)\text{Co}(\text{PMe}_3)_3]^{[47b]}$ (680 mg, 1.32 mmol) in THF (30 mL) was stirred under 1 bar of carbon monoxide for 3 h at 20 °C to form an olive green solution. The supernatant solution was decanted and kept at -27 °C to afford green crystals of **13**. The solid was recrystallized from diethyl ether/THF (1:4). Combined yield: 252 mg (41%); m.p. 155–157 °C (dec.). IR (Nujol, KBr): $\tilde{\nu} = 1876$ [vs, (C=O)], 1577 (m), 1542 [w, (C=C)] cm^{-1} . ^1H NMR (500 MHz, $[\text{D}_8]\text{THF}$, 300 K): $\delta = 0.44$ (t', $^2J_{PH} + ^4J_{PH} = 8.1$ Hz, 18 H, PCH_3), 6.56 (dt, $^3J_{PH} = 4.5$, $^3J_{PH} = 6.8$, $^3J_{HH} = 14.1$ Hz, 1 H, Ar-H), 6.74 (dd, $^3J_{PH} = 4.5$, $^3J_{PH} = 6.8$, $^3J_{HH} = 14.1$ Hz, 1 H, Ar-H), 6.95 (dd, $^3J_{PH} = 4.5$, $^3J_{PH} = 6.8$, $^3J_{HH} = 14.1$ Hz, 1 H, Ar-H), 7.13 (dd, $^3J_{PH} = 4.5$, $^3J_{PH} = 6.8$, $^3J_{HH} = 14.1$ Hz, 1 H, Ar-H), 7.29 (dd, $^3J_{PH} = 4.5$, $^3J_{PH} = 6.8$, $^3J_{HH} = 14.1$ Hz, 1 H, Ar-H), 7.34 (dd, $^3J_{PH} = 4.5$, $^3J_{PH} = 6.8$, $^3J_{HH} = 14.1$ Hz, 1 H, Ar-H), 7.60 (dd, $^3J_{PH} = 4.5$, $^3J_{PH} = 6.8$, $^3J_{HH} = 14.1$ Hz, 1 H, Ar-H), 8.75 (d, $^3J_{HH} = 7.8$ Hz, 1 H, NCH) ppm. $^{13}\text{C}\{^1\text{H}\}$ NMR (125 MHz, $[\text{D}_8]\text{THF}$, 300 K): $\delta = 13.4$ (t', $^1J_{PC} + ^3J_{PC} = 26.3$ Hz, PCH_3), 109.4 (d, $^3J_{PC} = 5.0$ Hz, CH), 115.9 (s, CH), 116.5 (s, CH), 117.8 (d, $^3J_{PC} = 5.0$ Hz, CH), 121.8 (s, CH), 122.3 (s, CH), 122.7 (s, CH), 130.8 (s, C), 133.7 (s, CH), 134.6 (dd, $^3J_{PC} = 11.3$, $^3J_{PC} = 5.0$ Hz, CH), 147.7 (d, $^3J_{PC} = 6.3$ Hz, C), 149.8 (s, C), 151.2 (s, CH), 166.7 (s, NC), 183.3 (m, Fe-C), 211.3 (m, Fe-C), 234.3 (m, Fe-CO) ppm. $^{31}\text{P}\{^1\text{H}\}$ NMR (202 MHz, $[\text{D}_8]\text{THF}$, 203 K): $\delta = 21.1$ (s, 2 P, PCH_3)

ppm. $\text{C}_{24}\text{H}_{29}\text{FeNOP}_2$ (465.3): calcd. C 61.95, H 6.28, N 3.01; found C 61.49, H 6.15, N 2.98.

X-ray Crystallography: The data were collected at room temperature with the crystals under argon in glass capillaries; air-stable specimens were glued to a glass fiber. The data were collected by using the SMART software^[66] with a Bruker AXS SMART APEX CCD (University of Paderborn) diffractometer and a graphite monochromator with Mo- K_α radiation ($\lambda = 0.71073$ Å). A summary of the crystal data, data collection, and structure refinement is listed in Table 5. The data reductions were performed by using the SAINT software^[67] and the data were corrected for absorption by using SADABS.^[68] The structures were solved by direct and conventional Fourier methods^[69] and refined by full-matrix least-squares techniques on F^2 with anisotropic displacement parameters for the non-hydrogen atoms.^[69] The hydrogen atoms were refined at idealized positions riding on their parent atoms with isotropic displacement parameters $U_{\text{iso}}(\text{H}) = 1.2U_{\text{eq}}(\text{C})$ or $1.5U_{\text{eq}}(\text{methyl})$. All CH_3 hydrogen atoms were allowed to rotate but not to tip. For **5**, one severely disordered pentane solvent molecule was treated with the SQUEEZE facility of PLATON.^[70]

CCDC-1031297 (for **2**), -1031298 (for **3**), -1031299 (for **5**), -1031300 (for **6**), -1031301 (for **7**), -1031302 (for **8**), -1031303 (for **9**), -1031304 (for **11**), and -1031305 (for **12**) contain the supplementary crystallographic data for this paper. These data can be obtained free of charge from The Cambridge Crystallographic Data Centre via www.ccdc.cam.ac.uk/data_request/cif.

Calculations: Ab initio DFT calculations on **7** were performed with the Firey QC package,^[71] which is partially based on the GAMESS (US)^[72] source code, with the PBE1PBE functional,^[73] modified in its hybrid version by Adamo and Barone^[74] (this functional uses 25% exchange and 75% correlation weighting and is known as PBE0) and the modified three-parameter hybrid functional of Becke (B3)^[75] with the Lee, Yang, and Parr (LYP)^[76] expression for the nonlocal correlation provided by Perdew and Wang (B3PW91).^[77] Basis functions used the Ahlrichs TZVP basis set (triple zeta for valence electrons plus polarization function).^[78] Harmonic analysis at the same level of theory (PBE0/TZVP) was performed for all of the equilibrium geometries to confirm that they were minima, that is, that there were no imaginary frequencies, on the potential energy surface (PES). The molecular orbitals, optimized structures, and spin density pictures were created by the ChemCraft program.^[79]

Acknowledgments

Financial support of this work by Fonds der Chemischen Industrie is gratefully acknowledged.

- [1] a) M. Albrecht, *Chem. Rev.* **2009**, *110*, 576–623; b) D. A. Colby, R. G. Bergman, J. A. Ellman, *Chem. Rev.* **2009**, *110*, 624–655; c) J. A. Labinger, J. E. Bercaw, *Nature* **2002**, *417*, 507–514; d) A. E. Shilov, G. B. Shul'pin, *Chem. Rev.* **1997**, *97*, 2879–2932; e) C.-H. Jun, C. W. Moon, D.-Y. Lee, *Chem. Eur. J.* **2002**, *8*, 2422–2428; f) I. Omae, *Cyclometalation Reactions: Five-Membered Ring Products as Universal Reagents*, Springer, Tokyo, **2014**.
- [2] a) D. Vogt, B. Cornils, W. Herrmann, *Applied Homogeneous Catalysis with Organometallic Compounds*, volume 1, VCH Verlagsgesellschaft, Weinheim, Germany, **1996**; b) P. W. N. M van Leeuwen, *Homogeneous Catalysis: Understanding the Art*, Kluwer Academic, Dordrecht, The Netherlands, **2004**; c) F. Kakiuchi, in: *Topics in Organometallic Chemistry*, vol. 24: *Directed Metallation* (Ed.: N. Chatani), Springer, Berlin, **2007**, p.

- 1–33; d) H. U. Blaser, E. Schmidt (Eds.), *Asymmetric Catalysis on Industrial Scale: Challenges, Approaches and Solutions*, Wiley-VCH, Weinheim, Germany, **2011**.
- [3] a) P.-S. Lee, T. Fujita, N. Yoshikai, *J. Am. Chem. Soc.* **2011**, *133*, 17283–17295; b) K. Gao, N. Yoshikai, *Acc. Chem. Res.* **2014**, *47*, 1208–1219; c) L. Ackermann, *J. Org. Chem.* **2014**, *79*, 8948–8954; d) D. Tilly, G. Dayaker, P. Bachu, *Catal. Sci. Technol.* **2014**, *4*, 2756–2777.
- [4] I. Omae, *Coord. Chem. Rev.* **2004**, *248*, 995–1023.
- [5] a) G. Dyker, *Handbook of C–H transformations: Applications in: Organic Synthesis* vol. 2, Wiley-VCH, Weinheim, Germany, **2005**; b) J. Tsuji, *Transition Metal Reagents and Catalysts*, John Wiley & Sons, Chichester, UK, **2000**; c) I. Omae, *Appl. Organomet. Chem.* **2009**, *23*, 91–107.
- [6] a) M. Hanif, Z. H. Chohan, *Appl. Organomet. Chem.* **2013**, *27*, 36–44; b) S. Blanck, T. Cruchter, A. Vultur, R. Riedel, K. Harms, M. Herlyn, E. Meggers, *Organometallics* **2011**, *30*, 4598–4606; c) C. G. Hartinger, P. J. Dyson, *Chem. Soc. Rev.* **2009**, *38*, 391–401; d) S. M. Meier, M. Hanif, Z. Adhireksan, V. Pichler, M. Novak, E. Jirkovsky, M. A. Jakupc, V. B. Arion, C. A. Davey, B. K. Keppler, C. G. Hartinger, *Chem. Sci.* **2013**, *4*, 1837–1846; e) R. Breslow (Ed.), *Artificial Enzymes*, Wiley-VCH, Weinheim, Germany, **2006**.
- [7] a) W.-Y. Wong, Z. He, S.-K. So, K.-L. Tong, Z. Lin, *Organometallics* **2005**, *24*, 4079–4082; b) F. Gao, Y. Wang, D. Shi, J. Zhang, M. Wang, X. Jing, R. Humphry-Baker, P. Wang, S. M. Zakeeruddin, M. Grätzel, *J. Am. Chem. Soc.* **2008**, *130*, 10720–10728; c) G. Ge, J. He, H. Guo, F. Wang, D. Zou, *J. Organomet. Chem.* **2009**, *694*, 3050–3057.
- [8] G. Zhou, W.-Y. Wong, X. Yang, *Chem. Asian J.* **2011**, *6*, 1706–1727.
- [9] a) L. Ilies, J. Okabe, N. Yoshikai, E. Nakamura, *Org. Lett.* **2010**, *12*, 2838–2840; b) L. Ilies, S. Asako, E. Nakamura, *J. Am. Chem. Soc.* **2011**, *133*, 7672–7675.
- [10] a) R. M. (Ed.) Bullock, *Catalysis without Precious Metals*, Wiley-VCH, Weinheim, Germany, **2010**; b) R. B. King (Ed.), *Encyclopedia of Inorganic Chemistry*, John Wiley, Chichester, UK, **1994**.
- [11] J. Hagen, *Industrial Catalysis: A Practical Approach*, Wiley-VCH, Weinheim, Germany, **2006**.
- [12] a) R. Beck, M. Frey, S. Camadanli, H.-F. Klein, *Dalton Trans.* **2008**, 4981–4983; b) R. Beck, H. Sun, X. Li, H.-F. Klein, *Z. Anorg. Allg. Chem.* **2009**, *635*, 99–105; c) R. Beck, U. Flörke, H.-F. Klein, *Inorg. Chem.* **2009**, *48*, 1416–1422; d) S. Camadanli, R. Beck, U. Flörke, H.-F. Klein, *Dalton Trans.* **2008**, 5701–5704; e) R. Beck, H. Sun, X. Li, S. Camadanli, H.-F. Klein, *Eur. J. Inorg. Chem.* **2008**, 3253–3257; f) R. Beck, T. Zheng, H. Sun, X. Li, U. Flörke, H.-F. Klein, *J. Organomet. Chem.* **2008**, *693*, 3471–3478.
- [13] S. Camadanli, R. Beck, U. Flörke, H.-F. Klein, *Organometallics* **2009**, *28*, 2300–2310.
- [14] H.-F. Klein, S. Camadanli, R. Beck, D. Leukel, U. Flörke, *Angew. Chem. Int. Ed.* **2005**, *44*, 975–977; *Angew. Chem.* **2005**, *117*, 997.
- [15] a) K. R. Flower, V. J. Howard, R. G. Pritchard, J. E. Warren, *Organometallics* **2002**, *21*, 1184–1189; b) K. R. Flower, L. G. Leal, R. G. Pritchard, *J. Organomet. Chem.* **2005**, *690*, 3390–3396; c) K. R. Flower, R. G. Pritchard, J. E. Warren, *Eur. J. Inorg. Chem.* **2003**, 1929–1938; d) B. Li, T. Roisnel, C. Darcel, P. H. Dixneuf, *Dalton Trans.* **2012**, *41*, 10934–10937; e) K. A. Azam, D. W. Bennett, M. R. Hassan, D. T. Haworth, G. Hogarth, S. E. Kabir, S. V. Lindeman, L. Salassa, S. R. Simi, T. A. Siddiquee, *Organometallics* **2008**, *27*, 5163–5166.
- [16] a) M. Crespo, C. M. Anderson, N. Kfoury, M. Font-Bardía, T. Calvet, *Organometallics* **2012**, *31*, 4401–4404; b) R. Martín, M. Crespo, M. Font-Bardía, T. Calvet, *Organometallics* **2008**, *28*, 587–597; c) M. Crespo, M. Font-Bardía, X. Solans, *J. Organomet. Chem.* **2006**, *691*, 444–454; d) M. Crespo, X. Solans, M. Font-Bardía, *Organometallics* **1995**, *14*, 355–364; e) J. Rodríguez, J. Zafrilla, J. Albert, M. Crespo, J. Granell, T. Calvet, M. Font-Bardía, *J. Organomet. Chem.* **2009**, *694*, 2467–2475; f) L. Keyes, T. Wang, B. O. Patrick, J. A. Love, *Inorg. Chim. Acta* **2012**, *380*, 284–290.
- [17] M. Martín, E. Sola, S. Tejero, J. L. Andrés, L. A. Oro, *Chem. Eur. J.* **2006**, *12*, 4043–4056.
- [18] G. R. Newkome, K. J. Theriot, B. K. Cheskin, D. W. Evans, G. R. Baker, *Organometallics* **1990**, *9*, 1375–1379.
- [19] A. G. Wong-Foy, L. M. Henling, M. Day, J. A. Labinger, J. E. Bercaw, *J. Mol. Catal. A* **2002**, *189*, 3–16.
- [20] a) R. Castro-Rodrigo, M. A. Esteruelas, S. Fuentès, A. M. López, S. Mozo, E. Oñate, *Organometallics* **2009**, *28*, 5941–5951; b) B. Eguillor, M. A. Esteruelas, M. Oliván, E. Oñate, *Organometallics* **2005**, *24*, 1428–1438.
- [21] a) L. Zhang, L. Dang, T. B. Wen, H. H. Y. Sung, I. D. Williams, Z. Lin, G. Jia, *Organometallics* **2007**, *26*, 2849–2860; b) J. N. Coalter, W. E. Streib, K. G. Caulton, *Inorg. Chem.* **2000**, *39*, 3749–3756; c) M. L. Buil, M. A. Esteruelas, E. Goni, M. Oliván, E. Oñate, *Organometallics* **2006**, *25*, 3076–3083.
- [22] J. Navarro, E. Sola, M. Martín, I. T. Dobrinovitch, F. J. Lahoz, L. A. Oro, *Organometallics* **2004**, *23*, 1908–1917.
- [23] M. A. Cinellu, F. Cocco, G. Minghetti, S. Stoccoro, A. Zucca, M. Manassero, *J. Organomet. Chem.* **2009**, *694*, 2949–2955.
- [24] T. Kobayashi, H. Yorimitsu, K. Oshima, *Chem. Asian J.* **2011**, *6*, 669–673.
- [25] S. Oi, K. Sakai, Y. Inoue, *Org. Lett.* **2005**, *7*, 4009–4011.
- [26] a) G. Jia, D. W. Meek, J. C. Gallucci, *Organometallics* **1990**, *9*, 2549–2555; b) O. V. Ozerov, M. Pink, L. A. Watson, K. G. Caulton, *J. Am. Chem. Soc.* **2004**, *126*, 2105–2113.
- [27] C. P. Lenges, M. Brookhart, B. E. Grant, *J. Organomet. Chem.* **1997**, *528*, 199–203.
- [28] a) H.-F. Klein, H. H. Karsch, *Chem. Ber.* **1975**, *108*, 944–955; b) M. Gass, *Ph. D. Thesis*, Darmstadt University of Technology, Germany, **1988**; c) J. R. Bleeke, B. L. Lutes, M. Lipschutz, D. Sakellariou-Thompson, J. S. Lee, N. P. Rath, *Organometallics* **2010**, *29*, 5057–5067.
- [29] A. W. Addison, T. N. Rao, J. Reedijk, J. van Rijn, G. C. Verschoor, *J. Chem. Soc., Dalton Trans.* **1984**, 1349–1356.
- [30] J.-P. Djukic, W. Iali, A. Hijazi, L. Ricard, *J. Organomet. Chem.* **2011**, *696*, 2101–2107.
- [31] F. H. Allen, *Acta Crystallogr., Sect. A* **2002**, *58*, 380–388.
- [32] a) H. Xu, W. H. Bernskoetter, *J. Am. Chem. Soc.* **2011**, *133*, 14956–14959; b) H. Xu, P. G. Williard, W. H. Bernskoetter, *Organometallics* **2013**, *32*, 798–806.
- [33] R. Beck, H.-F. Klein, *Z. Anorg. Allg. Chem.* **2008**, *634*, 1971–1974.
- [34] H. F. Klein, H. H. Karsch, *Inorg. Chem.* **1975**, *14*, 473–477.
- [35] S. W. Kohl, F. W. Heinemann, M. Hummert, H. Weißhoff, A. Grohmann, *Eur. J. Inorg. Chem.* **2006**, 3901–3910.
- [36] A. G. Orpen, L. Brammer, F. H. Allen, O. Kennard, D. G. Watson, R. Taylor, *J. Chem. Soc., Dalton Trans.* **1989**, S1–S83.
- [37] Y. Yu, J. M. Smith, C. J. Flaschenriem, P. L. Holland, *Inorg. Chem.* **2006**, *45*, 5742–5751.
- [38] M. A. Esteruelas, F. J. Fernández-Alvarez, M. Oliván, E. Oñate, *J. Am. Chem. Soc.* **2006**, *128*, 4596–4597.
- [39] H.-F. Klein, R. Beck, U. Flörke, H.-J. Haupt, *Eur. J. Inorg. Chem.* **2003**, 1380–1387.
- [40] a) P. Barrio, M. A. Esteruelas, E. Oñate, *Organometallics* **2004**, *23*, 3627–3639; b) F. Ortega-Jiménez, M. C. Ortega-Alfaro, J. G. López-Cortés, R. Gutiérrez-Pérez, R. A. Toscano, L. Velasco-Ibarra, E. Peña-Cabrera, C. Alvarez-Toledano, *Organometallics* **2000**, *19*, 4127–4133.
- [41] P. W. N. M. van Leeuwen, *Homogeneous Catalysis*, Kluwer Academic, Dordrecht, The Netherlands, **2004**, p. 1–19.
- [42] a) J. Foerster, A. Kakoschke, R. Goddard, J. Rust, R. Wartchow, H. Butenschön, *J. Organomet. Chem.* **2001**, *617*–618, 412–422; b) H. Wadepohl, W. Galm, H. Pritzkow, A. Wolf, *Chem. Eur. J.* **1996**, *2*, 1453–1465.
- [43] M. Barbasiewicz, A. Szadkowska, R. Bujok, K. Grella, *Organometallics* **2006**, *25*, 3599–3604.
- [44] H. J. Reich, *J. Chem. Educ.* **1995**, *72*, 1086.

- [45] G. R. Fulmer, A. J. M. Miller, N. H. Sherden, H. E. Gottlieb, A. Nudelman, B. M. Stoltz, J. E. Bercaw, K. I. Goldberg, *Organometallics* **2010**, *29*, 2176–2179.
- [46] a) S. I. Kozhushkov, J. Foerstner, A. Kakoschke, D. Stellfeldt, L. Yong, R. Wartchow, A. de Meijere, H. Butenschön, *Chem. Eur. J.* **2006**, *12*, 5642–5647; b) H.-F. Klein, R. Beck, U. Flörke, H.-J. Haupt, *Eur. J. Inorg. Chem.* **2002**, 3305–3312; c) S. Deblon, L. Liesum, J. Harmer, H. Schönberg, A. Schweiger, H. Grützmacher, *Chem. Eur. J.* **2002**, *8*, 601–611.
- [47] a) E. R. Bartholomew, E. C. Volpe, P. T. Wolczanski, E. B. Lobkovsky, T. R. Cundari, *J. Am. Chem. Soc.* **2013**, *135*, 3511–3527; b) H.-F. Klein, S. Camadanli, R. Beck, U. Flörke, *Chem. Commun.* **2005**, 381–382.
- [48] E. C. Volpe, P. T. Wolczanski, J. M. Darmon, E. B. Lobkovsky, *Polyhedron* **2013**, *32*, 406–415.
- [49] D. G. Johnson, J. M. Lynam, N. S. Mistry, J. M. Slattery, R. J. Thatcher, A. C. Whitwood, *J. Am. Chem. Soc.* **2012**, *135*, 2222–2234.
- [50] R. Beck, U. Flörke, H.-F. Klein, *Inorg. Chim. Acta* **2009**, *362*, 1984–1990.
- [51] C. M. Anderson, M. Crespo, N. Kfoury, M. A. Weinstein, J. M. Tanski, *Organometallics* **2013**, *32*, 4199–4207.
- [52] E. C. Volpe, P. T. Wolczanski, E. B. Lobkovsky, *Organometallics* **2009**, *29*, 364–377.
- [53] M. Brookhart, W. A. Chandler, A. C. Pfister, C. C. Santini, P. S. White, *Organometallics* **1992**, *11*, 1263–1274.
- [54] H. Schaeufele, D. Hu, H. Pritzkow, U. Zenneck, *Organometallics* **1989**, *8*, 396–401.
- [55] a) W. W. Brennessel, R. E. Jilek, J. E. Ellis, *Angew. Chem. Int. Ed.* **2007**, *46*, 6132–6136; *Angew. Chem.* **2007**, *119*, 6244; b) E.-M. Schnöckelborg, M. M. Khusniyarov, B. de Bruin, F. Hartl, T. Langer, M. Eul, S. Schulz, R. Pöttgen, R. Wolf, *Inorg. Chem.* **2012**, *51*, 6719–6730.
- [56] G. Zhu, J. M. Tanski, D. G. Churchill, K. E. Janak, G. Parkin, *J. Am. Chem. Soc.* **2002**, *124*, 13658–13659.
- [57] a) A. R. Dick, J. W. Kampf, M. S. Sanford, *Organometallics* **2005**, *24*, 482–485; b) N. Godbert, T. Pugliese, I. Aiello, A. Bellusci, A. Crispini, M. Ghedini, *Eur. J. Inorg. Chem.* **2007**, 5105–5111; c) D. E. Janzen, D. G. VanDerveer, L. F. Mehne, D. A. da Silva Filho, J.-L. Bredas, G. J. Grant, *Dalton Trans.* **2008**, 1872–1882; d) J. R. Berenguer, J. Fernández, N. Giménez, E. Lalinde, M. T. Moreno, S. Sánchez, *Organometallics* **2013**, *32*, 3943–3953; e) J. L. Serrano, L. García, J. Pérez, E. Pérez, J. García, G. Sánchez, G. López, M. Liu, *Eur. J. Inorg. Chem.* **2008**, 4797–4806; f) G. Sánchez, J. García, D. Meseguer, J. L. Serrano, L. García, J. Pérez, G. López, *Dalton Trans.* **2003**, 4709–4717; g) M. A. Esteruelas, F. J. Fernández-Alvarez, M. Oliván, E. Oñate, *Organometallics* **2009**, *28*, 2276–2284; h) T. Dubé, J. W. Faller, R. H. Crabtree, *Inorg. Chem.* **2002**, *41*, 5561–5565; i) D.-H. Lee, H. J. Kwon, B. P. Patel, L. M. Liable-Sands, A. L. Rheingold, R. H. Crabtree, *Organometallics* **1999**, *18*, 1615–1621; j) J. G. Małecki, M. Jaworska, R. Kruszynski, J. Kłak, *Polyhedron* **2005**, *24*, 3012–3021; k) J. Matthes, S. Gründemann, A. Toner, Y. Guari, B. Donnadieu, J. Spandl, S. Sabo-Etienne, E. Clot, H.-H. Limbach, B. Chaudret, *Organometallics* **2004**, *23*, 1424–1433.
- [58] A. Díez, J. Forníés, A. García, E. Lalinde, M. T. Moreno, *Inorg. Chem.* **2005**, *44*, 2443–2453.
- [59] S. Camadanli, *Ph. D. Thesis*, Darmstadt University of Technology, Germany, **2005**.
- [60] a) C. Zucchi, A. Cornia, R. Boese, E. Kleinpeter, H. Alper, G. Pályi, *J. Organomet. Chem.* **1999**, *586*, 61–69; b) H. Alper, L. Bencze, R. Boese, L. Caglioti, R. Kurdi, G. Pályi, S. Tiddia, D. Turrini, C. Zucchi, *J. Mol. Catal. A* **2003**, *204–205*, 227–233; c) C. Zucchi, R. Boese, K. Alberts, T. Herbrich, G. Tóth, L. Bencze, G. Pályi, *Eur. J. Inorg. Chem.* **2001**, 2297–2304.
- [61] a) C. Ni, P. P. Power, *Chem. Commun.* **2009**, 5543–5545; b) D. Benito-Garagorri, I. Lagoja, L. F. Veiros, K. A. Kirchner, *Dalton Trans.* **2011**, *40*, 4778–4792.
- [62] H. H. Karsch, *Chem. Ber.* **1977**, *110*, 2699–2711.
- [63] W. Wolfsberger, H. Schmidbaur, *Synth. React. Inorg. Met.-Org. Chem.* **1974**, *4*, 149–156.
- [64] E. W. Turnblom, T. J. Katz, *J. Am. Chem. Soc.* **1973**, *95*, 4292–4311.
- [65] a) C. J. Cavallito, H. S. Yun, J. C. Smith, F. F. Foldes, *J. Med. Chem.* **1969**, *12*, 134–138; b) M. J. Percino, V. Chapela, M. Salmón, G. Espinosa-Pérez, A. Herrera, A. Flores, *J. Chem. Crystallogr.* **1997**, *27*, 549–552.
- [66] SMART, *Molecular Analysis Research Tool*, Bruker AXS Inc., Madison, WI, **2001**.
- [67] SAINTPlus, *Data Reduction and Correction Program*, Bruker AXS Inc., Madison, WI, **2001**.
- [68] SADABS, *An Empirical Absorption Correction Program*, Bruker AXS Inc, Madison, WI, **2001**.
- [69] G. Sheldrick, *Acta Crystallogr., Sect. A* **2008**, *64*, 112–122.
- [70] A. Spek, *J. Appl. Crystallogr.* **2003**, *36*, 7–13.
- [71] A. A. Granovsky, *Firey*, version 7.1.G; <http://classic-chem.msu.su/gran/-games/index.html>.
- [72] M. W. Schmidt, K. K. Baldrige, J. A. Boatz, S. T. Elbert, M. S. Gordon, J. H. Jensen, S. Koseki, N. Matsunaga, K. A. Nguyen, S. Su, T. L. Windus, M. Dupuis, J. A. Montgomery, *J. Comput. Chem.* **1993**, *14*, 1347–1363.
- [73] J. P. Perdew, K. Burke, M. Ernzerhof, *Phys. Rev. Lett.* **1996**, *77*, 3865–3868.
- [74] C. Adamo, V. Barone, *J. Chem. Phys.* **1999**, *110*, 6158–6170.
- [75] A. D. Becke, *J. Chem. Phys.* **1993**, *98*, 5648–5652.
- [76] C. Lee, W. Yang, R. G. Parr, *Phys. Rev. B* **1988**, *37*, 785–789.
- [77] J. P. Perdew, Y. Wang, *Phys. Rev. B* **1992**, *45*, 13244–13249.
- [78] A. Schäfer, C. Huber, R. Ahlrichs, *J. Chem. Phys.* **1994**, *100*, 5829–5835.
- [79] G. A. Zhurko, *ChemCraft*, version 1.7 build 382; <http://www.chemcraftprog.-com>.

Received: March 1, 2015

Published Online: ■

Cyclometalated Compounds

R. Beck,* S. Camadanli, U. Flörke,

H.-F. Klein 1–18



Reactivity Diversification – Synthesis and Exchange Reactions of Cobalt and Iron 2-Alkenylpyridine/-pyrazine Complexes Obtained by Vinylic C(sp²)-H Activation

Keywords: C–H activation / Cyclometalation / Cobalt / Iron / Nitrogen heterocycles

